

Utility of Intravenous Curcumin Nanodelivery Systems for Improving *In Vivo* Pharmacokinetics and Anticancer Pharmacodynamics

Mahsa Bagheri, Cornelius F. van Nostrum, Robbert Jan Kok, Gert Storm, Wim E. Hennink, and Michal Heger*



Cite This: *Mol. Pharmaceutics* 2022, 19, 3057–3074



Read Online

ACCESS |

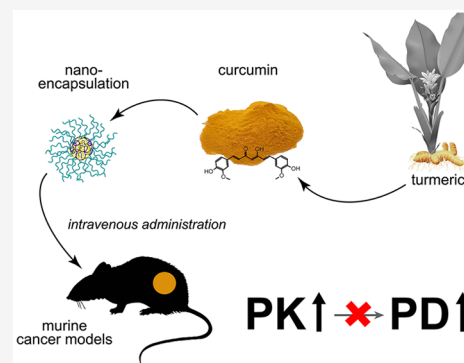
Metrics & More

Article Recommendations

Supporting Information

ABSTRACT: Curcumin nanoformulations for intravenous injection have been developed to offset poor absorption, biotransformation, degradation, and excessive clearance associated with parenteral delivery. This review investigates (1) whether intravenous nanoformulations improve curcumin pharmacokinetics (PK) and (2) whether improved PK yields greater therapeutic efficacy. Standard PK parameters (measured maximum concentration [C_{\max}], area under the curve [AUC], distribution volume [V_d], and clearance [CL]) of intravenously administered free curcumin in mice and rats were sourced from literature and compared to curcumin formulated in nanoparticles, micelles, and liposomes. The studies that also featured analysis of pharmacodynamics (PD) in murine cancer models were used to determine whether improved PK of nanoencapsulated curcumin resulted in improved PD. The distribution and clearance of free and nanoformulated curcumin were very fast, typically accounting for >80% curcumin elimination from plasma within 60 min. Case-matched analysis demonstrated that curcumin nanoencapsulation generally improved curcumin PK in terms of measured C_{\max} ($n = 27$) and AUC ($n = 33$), and to a lesser extent V_d and CL. However, when the data were unpaired and clustered for comparative analysis, only 5 out of the 12 analyzed nanoformulations maintained a higher relative curcumin concentration in plasma over time compared to free curcumin. Quantitative analysis of the mean plasma concentration of free curcumin versus nanoformulated curcumin did not reveal an overall marked improvement in curcumin PK. No correlation was found between PK and PD, suggesting that augmentation of the systemic presence of curcumin does not necessarily lead to greater therapeutic efficacy.

KEYWORDS: drug delivery, nanomedicine, micelles, nanoparticles, absorption, distribution, metabolism, excretion, cancer therapy



1. INTRODUCTION

Curcumin is a polyphenolic phytochemical derived from the rhizome of *Curcuma longa*. The crude root (turmeric) traditionally serves as a spice and dietary supplement.^{1,2} Curcumin, the principal bioactive constituent in turmeric, is considered for the prevention and treatment of numerous diseases and conditions owing to its advantageous pharmacological properties^{3–7} and clinical safety profile.^{8,9} The complete curcumin research spectrum is presented in Figure 1. Curcumin-related research has drastically intensified over the past decade, attesting to its widely perceived potential utility as an active pharmaceutical ingredient.

Curcumin is investigated as a cancer therapeutic in light of its apoptosis-inducing effects in hyperproliferative cells.^{11–14} However, the compound is pharmacodynamically (PD) fierce but pharmacokinetically (PK) weak when it comes to treatment of cancer.⁶ Curcumin inhibits more than 40 vital metabolic pathways in malignant cells as a result of pleiotropic interactions with biomolecules, ultimately causing apoptotic cell death.¹⁵ Non-to-low proliferative healthy cells remain

largely unaffected.^{16–18} Although proof-of-concept regarding curcumin's anticancer effects has been abundantly provided in mouse models of various types of human cancer,^{19,20} no notable therapeutic benefits have materialized in clinically approved and applied formulations.^{6,21} Two main reasons lie at the basis of this disconnect between animal research and clinical trials. First, many of the animal studies have been focused on systemically injected curcumin, while the vast majority of clinical studies hitherto have been conducted with orally dosed curcumin. Oral dosing gives rise to the second reason, which is that oral curcumin is associated with extremely low bioavailability^{9,22} due to poor intestinal absorption, extensive first-pass metabolism (phases I–III in enterocytes),

Received: June 6, 2022

Revised: August 3, 2022

Accepted: August 8, 2022

Published: August 16, 2022



curcumin nanoformulations to gauge their utility. Normalization to the plasma concentration measured several min after intravenous administration introduced some inaccuracy (i.e., overestimation) of the fraction of residual curcumin in the circulation that is equal to the “loss” of plasma curcumin during the time from injection to first measurement. This phenomenon only slightly impacts the amplitude but not the trend of the curve, which was predicated on actual plasma concentrations. When comparative analyses are performed, the vertical skewing of readouts could be minimized through protocol standardization (i.e., the time of first measurement is <5 min after curcumin injection).

In a separate analysis, normalized plasma concentrations of free curcumin and nanoencapsulated curcumin were fitted with a two-phase decay fit function to reflect distribution (KFast segment of the curve) and clearance (KSlow segment of the curve), corresponding to a two-compartment PK model. Fitting was performed on the entire measurement interval, which in some studies extended to 24 h postinjection. Given the rapid decay in curcumin plasma concentration, only the first 4 h postinjection is presented. It should be noted that these distribution and clearance phases theoretically represent a superimposed mixture of singular phases of the nanoparticles carrying the curcumin and the free curcumin that has exited the nanoparticle. Nonetheless, the singular phases of the curcumin nanoformulations were not parsed given their comparable pattern to free curcumin, indicating that the curcumin exited the nanoparticles during the first 5 min after injection and subsequently behaved as free curcumin (with the exception of a few formulations that better retained the curcumin cargo). Eleven of the 15 studies (73%) on free curcumin conformed to this model and yielded a goodness of fit (R^2) value of ≥ 0.9970 , whereas 12 of the 16 studies (73%) on nanoencapsulated curcumin yielded an R^2 value of ≥ 0.9912 . Finally, for comparative analysis, the normalized plasma concentrations of curcumin and nanoencapsulated curcumin were averaged per time point and the means \pm SD were plotted. The data points were fitted with a two-phase decay fit function.

The plasma curcumin concentration over time is typically analyzed by noncompartmental and compartmental models (section S2, Figures S1–S3). Among the common PK parameters, the maximum concentration (C_{\max}), area under the curve (AUC), and elimination half-life ($t_{1/2}$) are frequently reported. For purposes of simplicity, the C_{\max} values reported in this paper reflect the highest plasma concentration of curcumin at the earliest measured time point (1–15 min) and are therefore referred to as ‘measured C_{\max} ’. In our analysis, the C_{\max} definition therefore differs from the conventional definition used in the context of orally administered drugs. Conversely, only a few studies reported clearance (CL) and distribution volume (V_d), even though CL and V_d can be calculated from the plasma concentration–time curve.⁶⁵ In combination with AUC and $t_{1/2}$, these parameters indicate how quickly a compound is eliminated and reflect the propensity of the drug to stay in the circulation or distribute to other compartments.⁶⁶ The CL and V_d were therefore calculated using the data available for AUC and $t_{1/2}$ in instances where CL and V_d were not reported (see section S2 and Figure S4 for more detailed information). The V_d values were calculated when the values were not explicitly reported in the included studies. To enable interstudy comparative analysis of the PK parameters, values were converted to harmonize the units and

the AUCs were subsequently normalized to the administered curcumin dose and expressed as $(\mu\text{g}\cdot\text{h}/\text{L})/(\text{mg}/\text{kg})$. Readers should not that the definition of V_d for nanoencapsulated drugs may veer from the classical definition of V_d for drugs whose plasma data follow log–linear decay. Inasmuch as the curcumin concentration kinetics curves did not fundamentally differ between free curcumin and nanoencapsulated curcumin (with the exception of 5 nanoformulations), and as this parameter was chiefly used as a predicate for investigations on the PK–PD relationship, this technical difference in V_d definitions was acknowledged but discounted from the analyses. Semantics related to V_d did not distort the main conclusions.

Finally, the correlation between PK and PD was analyzed in GraphPad Prism. Specifically, the correlation between the nominal difference in the percentage of tumor growth inhibition (%TGI, y-axis variable) and (1) the AUC, (2) the administered dosage, and (3) the nanoformulated curcumin:free curcumin AUC ratio (x-axis variables) was determined. The difference in %TGI was stratified into nanoformulated curcumin versus control, free curcumin versus control, and nanoformulated curcumin versus free curcumin using the % TGI values as measured at the end of the experiment as input data (Figure S5). The actual %TGI was extrapolated from the respective figure or derived from the text. The data obtained from mouse and rat studies were clustered. Accordingly, the nominal difference in %TGI ranges from 0 to 100%, where 0% means that the intervention had no tumoricidal effect compared to the control group (buffer or empty carrier in case of nanoformulated/free curcumin comparisons to control, and free curcumin when comparing nanoformulated versus free curcumin). Similarly, a value of 100% means that the tumor had been completely eliminated at the end of the experiment. However, complete eradication or regression of tumors was not observed in any study. Correlation analysis for the first two variables (AUC and dosage) is straightforward and spurs the expectation that, given the anticancer properties of curcumin and the improved PK of nanoformulated curcumin, a positive relationship exists between AUC and dosage versus the nominal difference in %TGI. The correlation between the nominal difference in %TGI and the nanoformulated curcumin:free curcumin AUC ratio entailed a slightly different rationale. Studies were included where the curcumin nanoformulation AUC was greater than the AUC of the free curcumin control (i.e., nanoformulated curcumin:free curcumin ratio of >1), and where respective controls had been properly implemented in the experimental design. Subsequently, the nominal difference in %TGI was plotted of the nanoformulated curcumin versus vehicle/solvent control and of the free curcumin versus solvent control as a function of the nanoformulated curcumin:free curcumin AUC ratio. These data provided insight into the level of antitumor activity per degree of improved PK due to curcumin nanoencapsulation to assess the expectation that a positive correlation would be observed.

3. NANOFORMULATIONS IMPROVE MULTIPLE CURCUMIN PHARMACOKINETICS PARAMETERS COMPARED TO NONFORMULATED FREE CURCUMIN

3.1. Pharmacokinetics of Intravenously Administered Free Curcumin. Representative PK profiles of free curcumin

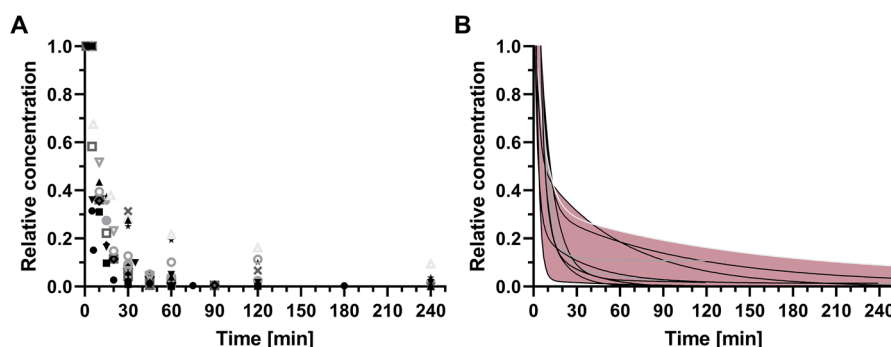


Figure 2. PK of free curcumin following intravenous administration in mice and rats as reported in literature. The x -axis and y -axis data were extracted from figures in published papers and verified by cross-referencing the text (where available). Plasma concentrations were normalized to the concentration measured at the earliest time point, not exceeding an interval of 5 min between injection and measurement. Normalized concentrations are provided in (A) as a function of circulation time. Data were compiled from 15 studies.^{43,48,49,51,53,54,56,60,61,63,64,70–73} The points were fitted with a two-phase decay fit function to reflect distribution (fast phase) and clearance (slow phase) (B). Eleven studies conformed to this PK model ($R^2 \geq 0.9970$).^{43,49,51,53,54,56,60,61,64,72,73} The maximum and minimum concentrations are represented by the outer bounds of the 11 fits (pink region). Compartmental deflection generally occurred between 20 and 30 min after intravenous administration.

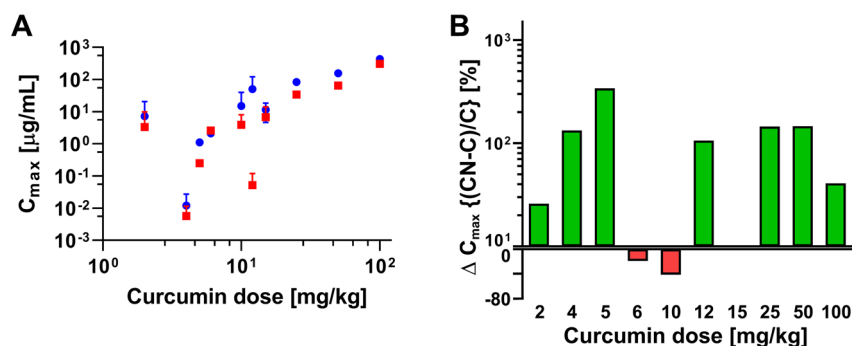


Figure 3. (A) Mean \pm SD measured C_{\max} of free curcumin (red square) and curcumin nanoformulations (blue circle) plotted as a function of injected dose in mice and rats ($n = 27$). (B) Fold-increase (green bars, log scale) and fold-decrease (red bars, linear scale) in the measured C_{\max} of nanoencapsulated curcumin relative to the measured C_{\max} of free curcumin, plotted as a percentage and as a function of injected curcumin dose. Abbreviations: Δ , delta (change); CN, curcumin nanoformulation; C, free curcumin.

in mice and rats are depicted in Figure 2. Plasma concentrations followed a biphasic pattern that is characterized by a rapid decay due to biodistribution and a slower decay due to elimination (Figure S1). More than 50% of the injected dose was no longer retrievable from plasma 10 min after administration, suggesting rapid tissue distribution. Curcumin is known to distribute to multiple organs, including the liver, kidneys, lungs, spleen, and brain^{42,49,56} and undergoes renal and hepatobiliary clearance.^{42,67–69} The switch from tissue distribution as the dominant cause of plasma decay to mainly clearance typically occurred between 20 and 30 min post-injection. At 30 min, only $13 \pm 10\%$ (mean \pm SD, $n = 14$) of the injected dose remained in the circulation and gradually dissipated during the subsequent 3–4 h.

Two key considerations should be pointed out in case of free curcumin. First, interspecies differences notwithstanding, the administered dose, type of solvent/vehicle, experimental design, and analytical method may differentially affect PK parameters.⁷⁴ This is illustrated by the rather wide relative concentration range per time point as presented in Figure 2. Some of the solvents/solubilizers that were used are micelle-forming surfactants (such as Kolliphore and Tween) that may prolong the systemic presence of curcumin. The consequences of curcumin solubilization by these excipients before or after intravenous administration on PK are further elaborated in section S3.1. Also, the possibility of assay interference should

be taken into account since some studies did not use chromatography-based equipment for effective compound separation. Second, with the therapeutic efficacy of intravenously administered free curcumin being relatively low (section 4), it is not difficult to fathom how therapeutically impotent orally dosed curcumin is in oncological patients. Bioavailability and therefore systemic concentrations are significantly hampered by the aforementioned absorption and metabolism issues (section 1) and ultimately yield systemic concentrations that are pharmacologically moot in an oncotherapeutic setting. These concerns have already been addressed for curcumin.⁷⁵ Nevertheless, for certain non-oncological indications (such as systematic inflammation, oxidative stress, etc.), the achieved plasma levels of oral curcumin are clinically adequate.⁷

3.2. Nanoencapsulation of Curcumin Improves the Measured C_{\max} in the Distribution Phase. For the analysis of measured C_{\max} (defined in section 2), 27 studies were included in which free and nanoencapsulated curcumin were administered intravenously into mice and rats at equal curcumin doses. For intravenously administered compounds, the measured C_{\max} corresponds to the highest concentration of compound in plasma detected immediately after injection, and in theory approximates the injected dose per mL blood.

As shown in Figure 2, the steep distribution phase of free curcumin typically lasts 20 min, followed by deflection into the

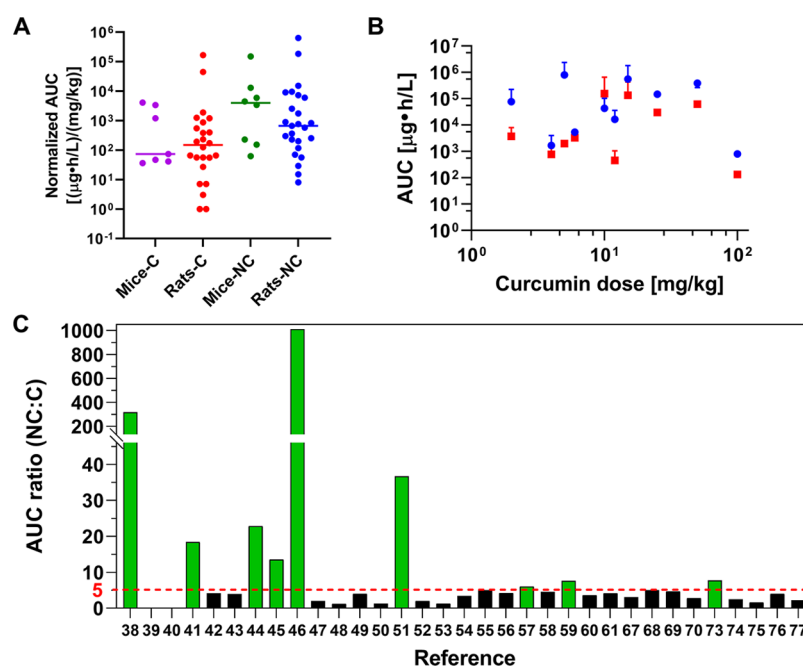


Figure 4. (A) Normalized AUC of free curcumin (C) and curcumin nanoformulations (NC) in mice and rats. Data were normalized to the injected dose. The horizontal line indicates the median. There is a significant difference between the normalized AUC values between the C and NC group in mice ($P = 0.031$) and rats ($P = 0.026$) (Mann–Whitney U test). (B) AUC of free curcumin (red square) and curcumin nanoformulations (blue circle) as a function of injected dose. (C) The AUC ratio of nanoformulated curcumin (NC) versus free curcumin (C) plotted per study in mice and rats. The dotted line represents a cutoff at an AUC ratio of ≥ 5 . Studies reporting an NC:C AUC ratio of ≥ 5 are indicated in green. No data were available for AUC of free curcumin in refs 41, 42, and 55.

shallower clearance phase. The range of the injection-measurement intervals was 1–15 min for the included studies.^{40–49,51–54,56,58–64,70–73,76–80} The measured C_{\max} values, stratified by injected dose, are presented in Figure 3A. The selected time frame allowed for the detection of PK differences between free curcumin and nanoencapsulated curcumin in the distribution phase only.

In line with expectations, the measured C_{\max} of curcumin increased with injected dose for both free and nanoformulated forms. However, the injected dose-measured C_{\max} relationship for nanoencapsulated curcumin (Spearman's $\rho = 0.909$; $p \leq 0.001$) showed a stronger correlation compared to the free form (Spearman's $\rho = 0.793$; $p \leq 0.01$) (Figure 3A). This dichotomy suggests that free curcumin exits the plasma compartment more profusely during the distribution phase than the curcumin contained in the nanoparticulate delivery systems. Of the 27 studies, the majority ($n = 19$) yielded a higher measured C_{\max} for the nanoformulations compared to the respective free form (Figure 3B). The increase in measured C_{\max} was around 100% for most dose comparisons. The data indicate that formulating curcumin into nanocarriers generally improves the measured C_{\max} and hence potential exposure of the tissues to the phytochemical compound (whether still encapsulated or released from the nanocarrier) during the distribution phase. Nevertheless, this is not a rule for every type of nanoparticulate carrier and the differential exposure also depends on the time interval between the injection and the first measurement time point, the curcumin release rate from the carrier, as well as the ability of the nanoparticles to extravasate and deliver the cargo into tumor cells such that cytotoxicity is conferred.

Currently it is not clear why the injected dose-measured C_{\max} correlation is stronger for nanoformulations than for the

free form and why nanoencapsulation improves the measured C_{\max} so considerably. The most plausible reason is that free curcumin rapidly settles into the membranes of blood cells upon entry into the systemic circulation,⁸¹ owing in part to its log P of 2.5.⁸² The mechanistic details that underlie curcumin-membrane interactions are provided elsewhere.^{83–85} This fraction of blood is not included in the plasma analysis, which does not apply to the cell-unassociated nanoparticulate curcumin that remains in the plasma fraction during sample processing. Another possibility is that hepatic and renal clearance already contribute to the concentration decline in the distribution phase and that the clearance favors free curcumin due to steric factors in terms of particle size relative to the size of the endothelial fenestrations in the kidneys and liver. Fast biliary clearance of free curcumin after intravenous injection, evidenced by the detection of curcumin in bile as early as 5 min after intravenous administration, was observed in rats.⁸⁶ Finally, free curcumin is more amenable to degradation in plasma than nanoencapsulated curcumin, where the excipient encapsulating curcumin offers protection chemically and/or sterically,^{37,87,88} culminating in comparatively lower retrieval of free curcumin from plasma. Hitherto no studies elaborately assessed the degradation rate of curcumin in a plasma matrix, and therefore the extent of this effect on the PK of curcumin is still unknown. It should be noted that, as was recently also demonstrated by our group,⁵⁵ most nanoparticulate curcumin carriers act as solubilizers and do not firmly retain the curcumin in the nanoparticle following systemic administration. Clearance of nanoparticulate curcumin is also quite steep during the distribution phase,^{43,48,49,51,53,54,56,60,61,63,64,70–73,76} albeit more delayed compared to free curcumin probably due to gradual release of curcumin from the nanoparticles.

3.3. Curcumin AUC Is Improved by Nanoencapsulation, but Not with Every Formulation Type. The AUC signifies a biological system's comprehensive exposure to a drug and, when juxtaposed to the PK curve (Figure 2), gives insights into the clearance rate of the drug. This parameter is instrumental in the analysis of different formulations in terms of their extent of drug exposure when administered at the same dose.⁸⁹ Curcumin is degraded in plasma⁹⁰ and rapidly removed from the circulation via renal and hepatic clearance^{42,67,69,86} and accumulation in various organs.⁹¹ This, together with the fact that curcumin is further metabolized and degraded in target cells,^{92,93} accounts for relatively brief PD activity after intravenous administration and accumulation in target tissue. Extending the circulatory presence (i.e., AUC) of curcumin by nanoencapsulation may therefore benefit PD efficacy. Moreover, the AUC is a better measure for pharmacological potency of the active principal than the measured C_{max} , particularly for intravenously administered drugs that are rapidly removed from the plasma compartment.

The AUC values of free and nanoencapsulated curcumin were derived from published studies in mice and rats. The AUC values were reported either as AUC_{0-t} ^{40,43,44,51,53,58,61,71} or $\text{AUC}_{0-\infty}$ ^{45-50,52,55-57,59,60,62-64,70,72,73,77-80}. Some studies did not specify the AUC reporting method.^{41,42,54,76} The AUCs were normalized to the injected dose (Tables S1–S4) and plotted (Figure 4A). Table 1 summarizes the range of

Table 1. Descriptive Statistics of Normalized AUC ($\mu\text{g}\cdot\text{h}/\text{L}/(\text{mg}/\text{kg})$) of Free Curcumin and Curcumin Nanoformulations in Mice and Rats^a

	free curcumin		curcumin nanoformulations	
	mice	rats	mice	rats
number of studies	7	23	9	24
minimum	36	1	62	8
maximum	4,075	167,000	149,705	632,000
median	73	171	4,482	714
mean	1,260	9,532	20,360	36,402
SEM	658	7,411	16,225	26,996

^aAbbreviation: SEM, standard error of the mean. The circulating blood volume is 78–80 mL/kg in mice and 50–70 mL/kg in rats.⁹⁴ Data assembled from refs 40–49, 51–64, 70–73, and 76–80. Statistical analysis of normalized AUC values between free curcumin and nanoencapsulated curcumin yielded a significant difference in mice ($P = 0.031$) and rats ($P = 0.026$); Mann–Whitney U test.

normalized AUC values for free curcumin and curcumin nanoformulations and provides the median and mean of the clustered data in both mice and rats. Notwithstanding the wide spread of normalized AUC values, a statistically significant difference was found between free versus nanoencapsulated curcumin AUC.

To determine whether data clustering, where dosing was discounted as variable, resulted in a misrepresentative AUC comparison, the AUC values were replotted as a function of the injected dose (Figure 4B). At all but one dosage the nanoformulated curcumin outperformed the free curcumin in terms of AUC. Also, the majority (22/31; 64%) of the studies revealed that curcumin nanoencapsulation augmented the AUC by a factor 1.3–5 compared to free curcumin (Figure 4C). Accordingly, the AUC improvements achieved by nanoencapsulation become masked in the normalized clustered

data (Figure 4B and C versus A). It also becomes clear that the type of nanoformulation plays a role in the extent of AUC improvement, addressed further in section 3.5.

As was performed for free curcumin (Figure 2), time–plasma concentration curves for nanoencapsulated curcumin were recreated from the published figures and cross-referenced with the text. The data are presented in Figure 5A,B and demonstrate that a substantial portion of curcumin nanoformulations was not effective in raising the relative plasma concentration of curcumin when compared to the free curcumin counterpart (Figure 2A). However, several formulations were able to protract the distribution → clearance deflection point beyond the 30 min threshold ($n = 6$) that was observed for free curcumin and maintain higher plasma levels of curcumin ($n = 5$). The 5 formulations exhibit two-phase decay traces that reside above the upper boundary of the kinetics traces of free curcumin (Figure 3B,C). Despite the 5 well-performing formulations, the overall average relative curcumin plasma concentration of the nanoformulations does not convincingly differ from that of free curcumin (Figure 5D), underscoring the fact that raising the AUC of curcumin and hence its potential PD efficacy relies heavily on formulation type.

In our recently published study on curcumin-loaded polymeric micelles composed of poly(ethylene glycol)-*b*-poly(*N*-2-benzoyloxypropyl methacrylamide) (mPEG-*b*-p-(HPMA-Bz)), we observed a notable incongruence between the PK of the carrier versus curcumin (see Figure 9 in ref 55). Twenty-four hours after intravenous administration, approximately 50% of the Cy-7-labeled mPEG-*b*-p-(HPMA-Bz) micelles was still present in the mouse circulation, whereas 90% of the loaded curcumin had been eliminated from the plasma compartment at 1 h postinjection. The curcumin elimination from plasma was likely facilitated by curcumin exiting the nanocarrier.

This brings about the following important matter: It is crucial to understand the underlying process of clearance of nanoformulated curcumin from plasma, which can stem from the systemic removal of the curcumin-containing nanocarrier as an intact drug-nanocarrier entity or from drug-nanocarrier destabilization in blood, causing release of the loaded curcumin and subsequent clearance of the released curcumin independently of the nanocarrier. The kinetics curves of curcumin nanoformulations presented in Figure 5B that resemble those of free curcumin in Figure 2B may reflect the latter process. A mechanistic understanding of the PK of nanoencapsulated curcumin is critical to appreciate the impact of nanocarriers on PD efficacy of curcumin inasmuch as two distinct scenarios are likely to happen. The unstable curcumin nanoformulation with comparable PK profile to that of free curcumin could either emulate the PD efficacy of free curcumin (rendering the nanocarrier nonadditive from a therapeutic standpoint) or improve the PD efficacy compared to the free curcumin. The latter phenomenon echoes other unstable nanoformulations such as Genexol and Abraxane. These nanoformulations exhibit a PK profile that is similar to nonencapsulated paclitaxel but yield superior therapeutic efficacy.^{95–97}

3.4. The Distribution Volume Is Positively Affected by Nanoencapsulation, but Depends on Formulation Type. The elimination of curcumin from plasma over time can have several causes. In addition to curcumin ending up in the discarded infranatant during sample processing (section 3.2), it may be metabolized and/or degraded,^{90,98} excreted

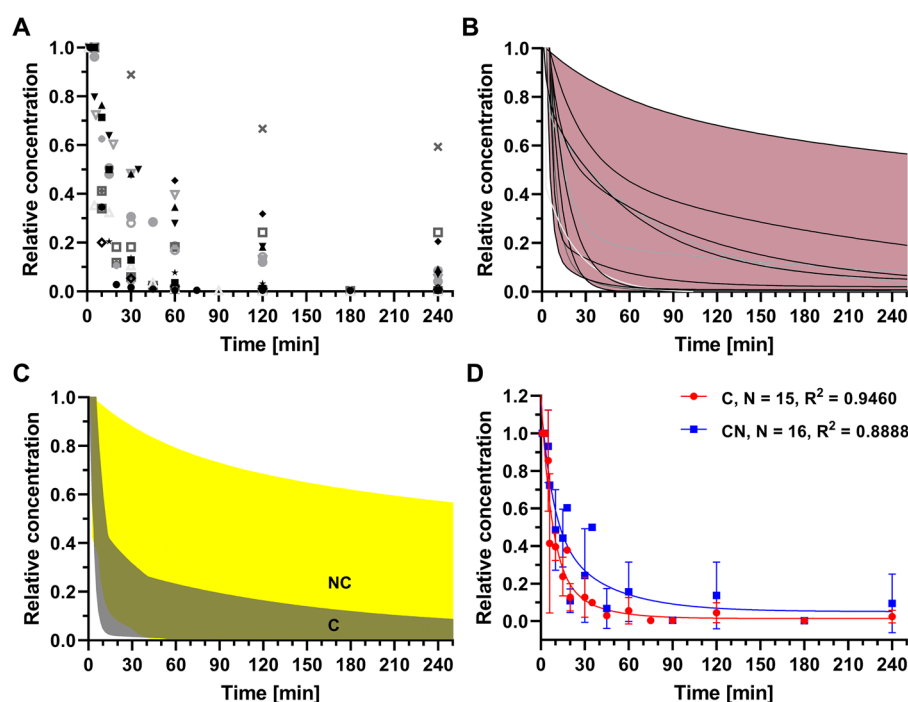


Figure 5. PK of nanoencapsulated curcumin following intravenous administration in mice and rats as reported in literature. The x-axis and y-axis data were extracted from published figures and verified by cross-referencing the text. Plasma concentrations were normalized to the concentration measured at the earliest time point, not exceeding an interval of 5 min between injection and measurement. Normalized concentrations are provided in (A) as a function of time after intravenous injection. Data were compiled from 15 studies.^{43,48,49,51,53,54,56,60,61,63,64,70–73} The points were fitted with a two-phase decay fit function to reflect distribution (fast phase) and clearance (slow phase) (B). Twelve studies conformed to this PK model ($R^2 \geq 0.9912$).^{43,48,49,51,53,60,63,64,70–73} The maximum and minimum concentration are represented by the outer bounds of the 12 fits (pink region). For some of the nanoformulations, compartmental deflection occurred between 10 and 30 min following intravenous administration. However, 6 formulations exhibited deflection points at >30 min after intravenous administration. The temporal spread in nanoformulated curcumin concentration (NC; B) was superimposed on that of free curcumin (C; Figure 2B) to show the pharmacokinetic and potential pharmacodynamic gain offered by curcumin nanoencapsulation (C), which applies mainly to the formulations where the traces in (B) course above the dark gray region designated as 'C' (formulation 1,⁶⁰ formulation 5,⁴³ and formulation 7⁵³ in Table 2 and refs 49 and 71). The relative plasma concentrations of free curcumin (Figure 2A) and nanoencapsulated curcumin (A) were averaged per time point and plotted as mean \pm SD as a function of time (D). The mean values were fitted with a two-phase decay fit function. The sample size and goodness of fit (R^2) values are reported in the top right.

renally and metabolized hepatically,^{42,67,69,86} or diffuse into the extravascular space (i.e., distribution into tissues^{91,99,100}). When considered in the context of oncopharmacology, the difference between renal/hepatic CL and tissue distribution is critical, whereby the former occurs at the detriment of PD efficacy. CL and distribution volume (V_d) can be calculated (section S2). The V_d represents the ratio of the amount of drug present in the body (injected dose) to the concentration of drug measured in plasma and is expressed as the volume of fluid required to be present in the extravascular space for achieving the concentration to be equivalent to the plasma concentration. The V_d correlates positively with the amount of drug distributed into tissue, is directly proportional to the lipophilicity of a compound, and inversely proportional to the extent of plasma retention.¹⁰¹

The V_d data are presented in Tables S1–S4. The calculated values, marked with an asterisk in Tables S1–S4, show the V_d at the terminal phase of elimination (schematically explained in Figure S1). The range of V_d values is very broad: 0.002–1,376 L/kg and 0.06–882 L/kg for free curcumin and nanoformulated curcumin, respectively. This spread can be due to variation in PK and differences in the V_d calculation method.⁶⁵ Two outlier studies^{57,64} reported unrealistic V_d values (2 and 4 mL/kg for free curcumin) that are far below the average blood volume in mice and rats (50–80 mL/kg or 7–8% body weight),^{102,103} casting doubt about the reliability of data

analysis. To provide perspective, the total body water:body weight ratio in mice is roughly 0.6 L/kg,¹⁰⁴ while the total plasma volume is approximately 49 mL/kg and extracellular water content is 232 mL/kg.¹⁰⁵ Additionally, the V_d of curcumin nanoformulations was lower,^{43–48,53,58,60,62,71,76} similar,^{50,72,77,78} or higher^{52,54,56,57,59,61,63,64,70,73,79,80} than free curcumin (Figure 6A). An NC:C V_d ratio of <1 indicates that curcumin was stably retained in the nanoparticles (and hence remained in the circulation), while a V_d of ≥ 1 suggests that the nanocarriers most likely acted as solubilizers with poor cargo retention, as addressed in section 3.3.

Duan et al.⁵⁷ and Ma et al.⁸⁰ observed a substantial increase in V_d for curcumin when loaded into chitosan/poly(butyl cyanoacrylate) nanoparticles and methoxy poly(ethylene oxide)-*block*-poly(ϵ -caprolactone) micelles, respectively. The authors postulated that this might be due to the sequestration of larger curcumin-loaded nanoparticles by cells of the reticuloendothelial system, which released curcumin and acted as a reservoir.

In regard to cancer treatment, a high V_d does not have to be detrimental to PD efficacy per se as long as the (nanoparticulate) curcumin predominantly accumulates in the target tissue to induce apoptosis of tumor cells. Exemplary proof-of-concept was recently provided by Rodell et al.,¹⁰⁶ who designed cyclodextrin-based nanoparticles encapsulating Toll-like receptor small molecular agonists intended to target to

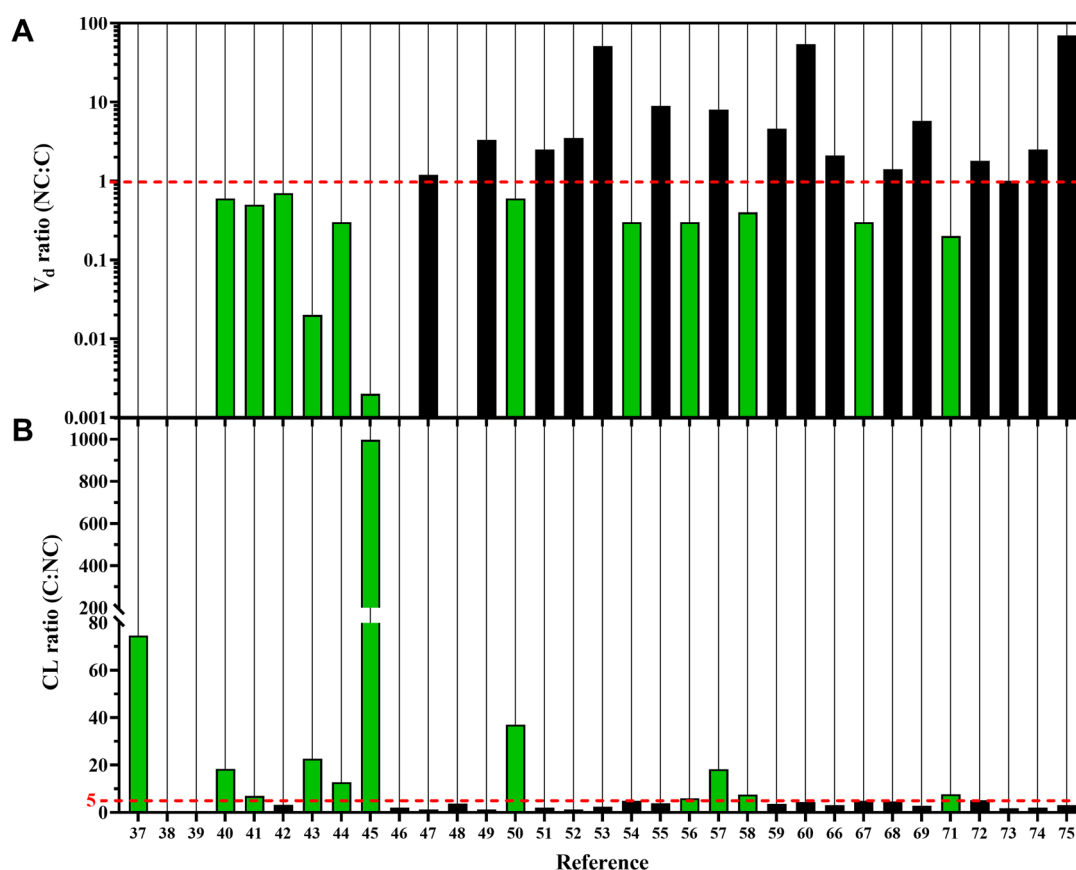


Figure 6. Distribution volume (V_d) ratio (A) and clearance (CL) ratio (B) of curcumin nanoformulations (NC) in relation to experiment-matched free curcumin (C) in mice and rats. The V_d ratio could not be calculated for refs 40–42, 49, 51, and 55 due to insufficient data. An NC:C V_d ratio of <1 (green bars) and a C:NC CL ratio of >5 (green bars) indicate that the NC formulations were better retained in plasma than free curcumin. The dotted line in (B) represents a cutoff at an AUC ratio of ≥ 5 . The references in (B, x-axis) are imposable on (A).

tumor-associated macrophages to steer their polarization and improve cancer immunotherapy efficacy. The drug-bearing nanoparticles accumulated most profoundly in the tumor tissue compared to the other 11 noncancerous tissues measured, which resulted in superior tumoricidal effects versus the nonencapsulated drug, despite distribution into off-target tissues. This not only contextualizes the practical significance of the V_d but also underscores the importance of including experiments focused on curcumin biodistribution, or at least curcumin accumulation in target tissue. Moreover, a sizable V_d can potentially be offset with efficient tumor targeting tools conferred on the drug delivery system.¹⁰⁷

CL represents the volume of plasma from which a substance is removed per unit time. As opposed to excretion, which strictly reflects the compound leaving the body through urine, feces, and sweat, CL is a measure of plasma disappearance rate and may encompass excretion when measurements are based solely on plasma levels. V_d and CL are closely related in that both metrics provide an indication of the amount of substance remaining in the circulation at or after a certain time. Accordingly, the C:NC CL ratios plotted in Figure 6B roughly reflect the V_d ratios portrayed in Figure 6A, attesting to the fact that 8 of 31 formulations^{43,46–48,53,60,62,76} were clearly capable of better retaining curcumin in the circulation and thereby increased the statistical probability that the encapsulated curcumin could reach and accumulate in a tumor exploiting the enhanced permeation and retention effect.^{108,109} The 9 nanoformulations that consistently outperformed free curcu-

min on the basis of AUC (Figure 4C), V_d (Figure 6A), and CL (Figure 6B) are highlighted in Table 2, with their compositional attributes and physicochemical characteristics discussed in the next section.

3.5. Physicochemical Characteristics of Curcumin Nanoformulations with Improved Pharmacokinetic Profiles. Studies on the well-performing formulations reported nanoformulated curcumin:free curcumin (NC:C) AUC ratios of 6, 7.6, 7.7, 13.5, 19, 23, and 37,^{43,46,47,53,60,62,76} where Sun et al.⁴⁰ and Yoon et al.⁴⁸ even obtained NC:C AUC ratios of 300 and 1,000, respectively (Figure 4C, green bars). The outstanding AUC values were also reflected in the V_d and CL (Figure 6, green bars). The type of nanoparticles and the physicochemical properties of these formulations are summarized in Table 2. The mean particle size ranged from 27 to 210 nm for the studies that reported an NC:C AUC ratio of >5 ,^{40,43,46–48,53,60,62,76} which is appropriate for prolonged circulation time.¹¹⁰ Moreover, the mean ζ potential of the particles was near-neutral (2.9 to -5.3 mV)^{48,53,62,76} or negative (<-10 mV).^{40,46,47}

The reasons given for the improved AUC of curcumin nanoformulations compared to free curcumin in terms of physicochemical characteristics (Table 2) have mainly been attributed to improved chemical stability of curcumin by encapsulation and retention inside the nanoparticle. For instance, Liu et al.⁴⁶ explained that higher micellar stability and better payload retention by the cross-linked micelles resulted in lower clearance of curcumin and thus a higher

Table 2. Summary of the Physicochemical Properties of Intravenously Administered Curcumin Nanoformulations with an AUC Ratio of >5 Compared to Free Curcumin (NC:C)^a

curcumin nanoformulation	mean size (nm)	mean ZP (mV)	loading capacity (%)	release profile	free curcumin vehicle	species	ID (mg/kg)	AUC ratio NC:C	ref
<i>Formulation 1:</i> mPEG-PCL ^b	27	NA	13	54.6% of total curcumin release within 9 days in PBS + 0.5% Tween 80 at pH = 7.4	Cremophor EL and dehydrated alcohol (1:1, v/v)	SD rats	100	6.0	60
<i>Formulation 2:</i> mPEG-PLA ^c	70	2.9	4.8	85% curcumin release after 96 h in physiological saline containing 1% Tween 80	DMA + PEG + glucose	rats	15	7.6	62
<i>Formulation 3:</i> mPEG-PCL ^b	30	−3.5	10	44.5% curcumin release after 100 h in PBS + 0.5% Tween 80 at pH = 7.4	NA	rats	50	7.7	76
<i>Formulation 4:</i> HA-curc-NC ^d	161	−2.5	3.3	15% release in PBS + 0.5% Tween at pH = 5.0. The release increased in the presence of HAase over 24 h. 40%, 60%, and 80% release within 24 h in PBS + 0.5% Tween containing 0.3 μ M HAase at pH = 7.4 (blood), 6.5 (cancer site), and 5.0 (lysosome), respectively.	NA	SD rats	2	13.5	47
<i>Formulation 5:</i> mPEG-PLGA nanoparticles ^e	120	NA	NA	70% release within 27 h in PBS at pH = 5.8. Release reached 90% in 144 h	NA	SD rats	4	19	43
<i>Formulation 6:</i> mPEG-b-PHEMA-SHA micelles ^f	104	−19	17.8	90% and 80% release after 30 h in PBS at pH = 7.4 for noncross-linked and cross-linked micelles, respectively. Higher release (35%) for pH-sensitive cross-linked micelles in acidic environment (pH = 5.0) was observed compared to noncross-linked micelles (25%).	NA	SD rats	5	23	46
<i>Formulation 7:</i> Zein-PSBMA micelles ^g	155	−5.3	3.6	77% curcumin release in PBS, pH = 7.4, after 168 h.	saline with 1% Tween 20	BALB/c mice	2	37	53
<i>Formulation 8:</i> HA-Cur-liposomes ^h	210	−37	13.2	100% release after 100 h in PBS + 0.2% Tween 80 at pH = 7.4	DMSO	BALB/c mice	10	317	40
<i>Formulation 9:</i> PDLGA-G-based nanoparticles ⁱ	200	−0.8	NA	10% and 45% release after 168 h in PBS at pH = 7.4 and pH = 5.5, respectively, as a result of polymer degradation and higher stability of curcumin at acidic pH	37.5% PEG 400 v/v	SD rats	12	1,011	48

^aAbbreviations: ZP, ζ potential; ID, injected dose; DMSO, dimethyl sulfoxide; DMA, dimethylacetamide; HA, hyaluronic acid; NA, not available; NC:C, curcumin nanoformulation:free curcumin; PBS, phosphate-buffered saline; PEG, polyethylene glycol; SD, Sprague–Dawley. ^bNanoformulation: monomethoxy poly(ethylene glycol)-poly(3-caprolactone). ^cNanoformulation: poly(ethylene glycol)-poly(lactic acid). ^dNanoformulation: hyaluronic acid-coated curcumin nanocrystals. ^eNanoformulation: (polyethylene glycol)-poly(lactic-co-glycolic acid). ^fNanoformulation: pH-responsive reversibly cross-linked micelles composed of poly(ethylene glycol)-b-poly(2-methacrylate ethyl 5-hexynoate). ^gNanoformulation: zein-poly(sulfobetaine methacrylate). ^hNanoformulation: hyaluronic acid-modified liposomes. ⁱNanoformulation: poly(D,L-lactic acid)-glycerol-based nanoparticles.

Table 3. Summary of the Therapeutic Efficacy Studies of Intravenously Administered Curcumin Nanoformulations^a

curcumin nanoformulation	mean size (nm)	mean ZP (mV)	animal model PK	animal model, xenograft PD	curcumin dosing schedule	monitoring time (d)	AUC ratio NC:C	%TGI (NC)	%TGI (C)	ref
curcumin-PBCA nanoparticles ^b	200	29	SD rats	athymic BALB/c nude mice, HepG2, s.c. flank	3 times per week for 28 days (curcumin dose unknown)	28	3.4	55	NA	57
mPEG-PLA micelles ^c	30	−0.3	SD rats	BALB/c mice, CT26 s.c. flank	50 mg/kg every 3 days for 15 days (total dose: 300 mg/kg)	25	5.0	80	60	58
mPEG-PCL-Phe(Boc) micelles ^d	23	NA	ICR mice	BALB/c nude mice, K562/ADR s.c. arm pit	40 mg/kg daily for 21 days (total dose: 840 mg/kg)	21	3.1	65	NA	70
mPEG-PCL micelles ^e	27	−0.8	C57BL/6 mice	LL/2 s.c. flank and pulmonary metastases i.v.	25 mg/kg every 2 days for 14 days (total dose: 200 mg/kg)	28	5.0	52	30	71
mPEG-PLA-PAE micelles ^f	pH = 7.4, 171; pH = 5.5, 23	pH = 7.4, 4; pH = 5.5, 25	BALB/c nude mice	BALB/c nude mice, MCF-7 s.c. flank	40 mg/kg on days 0, 2, 4, 6, and 8 (total dose: 200 mg/kg)	25	NA	65	NA	41
mPEG-PCL micelles ^e	27	NA	SD rats	BALB/c mice, C26 s.c.	25 mg/kg daily for 10 days (total dose: 250 mg/kg)	18	6.0	50	30	60
mPEG-b-PHEMA-SHA micelles ^g	104	−19	SD rats	BALB/c mice, 4T1 s.c.	20 mg/kg every 3 days for 21 days (total of 5 injections) (total dose: 100 mg/kg)	21	23	40	25	46
HA-curc-NC ^h	162	−25	SD rats	BALB/c mice, 4T1 s.c. flank breast	5 mg/kg every 2 days for 10 days (total dose: 30 mg/kg)	10	13.5	75	20	47
curcumin nanosuspension stabilized by mPEG-DSPE and SPC ⁱ	186	−19	SD rats	ICR mice, H22 s.c. ampit	10 mg/kg every other day (total dose: 40 mg/kg)	6	4.5	60	15	61
mPEG-PCL micelles ^e	30	−4	rats	BALB/c mice, CT26 s.c. flank	50 mg/kg every 2 days (total dose: 500 mg/kg)	18	7.7	20	16	76
HSA nanoparticles ^j	132	−21	rats	BALB/c mice, HT-29 s.c. dorsal flank	10 mg/kg every other day for 10 days (total dose: 60 mg/kg)	20	2.5	45	18	77

^aThe percentage of tumor growth inhibition (%TGI) is calculated as the difference in the ratio of tumor volume in the treatment group receiving curcumin nanoformulation compared to the untreated control group (%TGI (NC)) or the difference in the ratio of tumor volume of the treatment group receiving free curcumin versus the untreated control group (%TGI (C)) on the last day of tumor monitoring. Abbreviations: ZP, ζ potential; PK, pharmacokinetics; PD, pharmacodynamics; d, days; NC, curcumin nanoformulation; C, free curcumin; TGI, tumor growth inhibition; ref., reference; NA, not available; s.c., subcutaneous; i.v., intravenous. Cell lines: HepG2, human hepatocellular carcinoma; CT26, mouse fibroblasts from colon carcinoma; K562/ADR, human chronic myelogenous leukemia with selected resistance to doxorubicin; LL/2, mouse Lewis lung carcinoma; MCF-7, human mammary gland carcinoma; C26, mouse colon carcinoma; 4T1, mouse mammary gland carcinoma; H22, mouse hepatocellular carcinoma; HT-29, human colorectal adenocarcinoma. ^bNanoformulation: cationic poly(butyl) cyanoacrylate (PBCA) nanoparticles coated with chitosan. ^cNanoformulation: monomethoxy poly(ethylene glycol)-*block*-poly(ethylene glycol)-*block*-poly(ε-caprolactone) and *N*-(*tert*-butoxycarbonyl)-*L*-phenylalanine end-capped. ^dNanoformulation: methoxy poly(ethylene glycol)-*block*-poly(ε-caprolactone). ^eNanoformulation: methoxy poly(ethylene glycol)-*block*-poly(ε-caprolactone). ^fNanoformulation: pH-sensitive methoxy poly(ethylene glycol)-poly(lactide)-poly(β-amino ester). ^gNanoformulation: pH-responsive reversibly cross-linked micelles poly(ethylene glycol)-*b*-poly(2-methacrylate ethyl 5-hexynoate). ^hNanoformulation: hyaluronic acid-modified curcumin nanocrystals; ⁱcurcumin nanosuspension stabilized by mPEG2000-DSPE and soybean lecithin. ^jNanoformulation: human serum albumin nanoparticles.

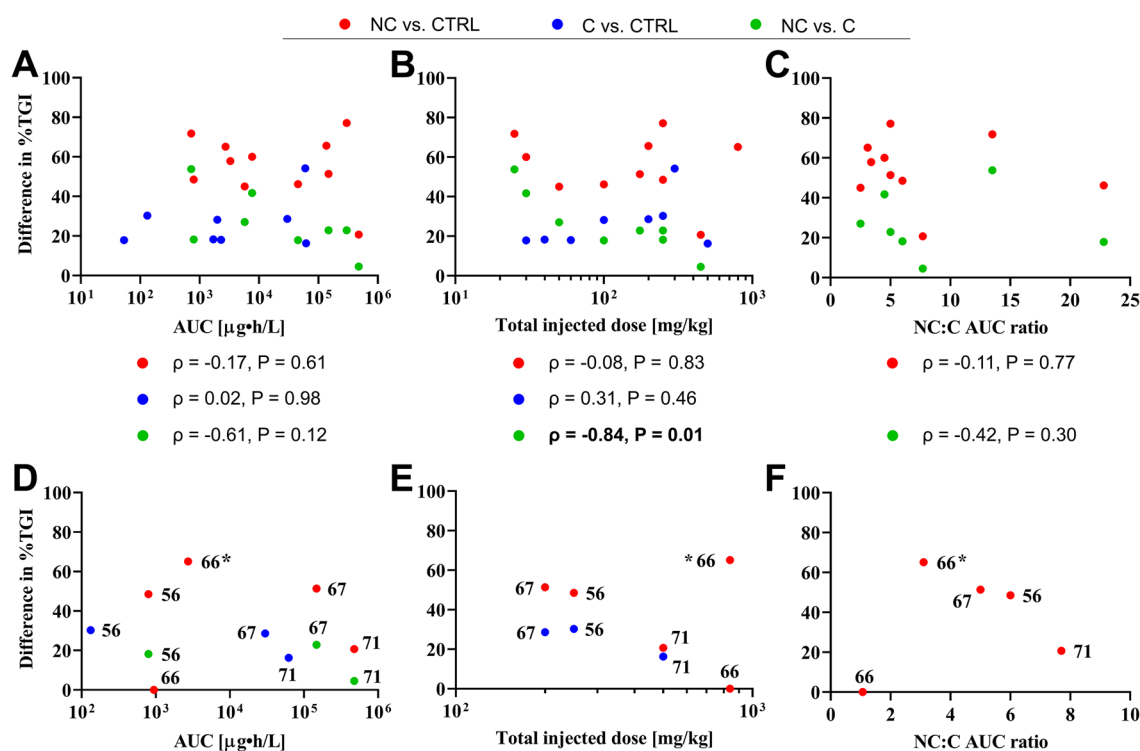


Figure 7. Correlation between therapeutic efficacy and AUC (A), total injected dose (B), and the nanoformulation curcumin:free curcumin (NC:C) ratio (C). The percentage of tumor growth inhibition (%TGI, y-axis) is provided as the nominal difference between %TGI of one group compared to another group (see legend), measured on the last day of tumor monitoring. The x-axis values in (A, B) pertain to NC (red circle, green circle) and C (blue circle) in the comparisons. The statistics (Spearman correlation coefficient, ρ , and P-value) of each comparison (legend) are presented below the panels. Panels (D–F) represent the same data sets as panels (A–C) but for curcumin-loaded mPEG-PCL micelles and free curcumin. The number next to each data point indicates the reference from which the data were collected.

AUC. However, the authors did not report the $t_{1/2}$ of these nanoparticles. Ji et al.⁴⁷ argued that hyaluronic acid (HA) grafting onto curcumin nanocrystals using 1-ethyl-(3-dimethyl aminopropyl) carbodiimide improved particle stability and slowed down curcumin release (100% curcumin release within 1 h and 15% within 24 h in PBS + 0.5% Tween, pH = 5.0, for uncoated and HA-coated curcumin nanocrystals, respectively). Similarly, the long-circulating property of zein-poly(sulfobetaine methacrylate) micelles (zein-PSBMA) (half-life not reported) composed of zein (a protein extracted from corn) as the core and poly(sulfobetaine methacrylate) as the shell, in addition to the high retention of the loaded curcumin, resulted in a 37 times greater NC:C AUC ratio.⁵³ Furthermore, sustained curcumin release from poly(D,L-lactic acid)-glycerol (PDLLA-G)-based nanoparticles was posited by Yoon et al.⁴⁸ to account for the high NC:C AUC ratio. Generally, the improved PK of intravenously administered nanoformulations relies on the stability and low clearance rate of the nanoparticles, ensuring high cargo retention and prolonged circulation time, rather than on a sustained release mechanism. In this study⁴⁸ with the highest reported NC:C AUC ratio of 1,000, the measured C_{max} of free curcumin was $\sim 0.1 \mu\text{g/mL}$ compared to $100 \mu\text{g/mL}$ for the nanoformulation at an equal injection dose of 12 mg/kg. Thus, it is likely that the high NC:C AUC ratio mainly resulted from the low AUC of free curcumin than from an extraordinary stability of the carrier system.

Of the studies that reported a high NC:C AUC ratio (Table 2), three studies performed *in vivo* imaging using a fluorescent tracer either encapsulated in or conjugated to the nanocarrier

to assess circulation time. DIR-loaded cross-linked mPEG-*b*-PHEMA-SHA micelles (Table 2, Formulation 6) showed prolonged circulation time and higher tumor accumulation compared to the non-cross-linked micelles and free dye as controls.⁴⁶ A drawback is that the *in vivo* imaging of DIR-loaded cross-linked mPEG-*b*-PHEMA-SHA micelles was performed in tumor-bearing mice, while the PK analysis was conducted in healthy rats. It is also remarkable that two HA-coated formulations^{40,47} were associated with a relatively high NC:C AUC ratio despite the fact that intravenously administered HA has a $t_{1/2}$ of 2.5–4.5 min.¹¹¹ Nonetheless, improved PK of nanoencapsulated curcumin has been ascribed to different types of HA-grafted nanoparticles. For instance, healthy mice received an intravenous injection of HA-coated liposomes loaded with DID (Table 2, Formulation 8), a lipophilic near-infrared fluorescent membrane dye, and were terminated after 12 h to select the optimal formulation in terms of HA molecular weight and grafting density based on organ uptake (especially the liver and spleen).⁴⁰

Attachment of HA is not strictly necessary. HA-lacking Cy5.5-labeled zein-PSBMA micelles (Table 2, Formulation 7) showed more intense fluorescence than the control group (free Cy5.5) and the fluorescence signal was detectable 72 h after injection in mice. In contrast, the control group exhibited a significant decrease in the fluorescence after 6 h followed by signal disappearance after 48 h, indicating prolonged circulation of zein-PSBMA micelles.⁵³ There are several stable nanoformulations with curcumin release of only $\sim 20\%$ after 24 h that yielded NC:C AUC ratios in the range of 4.1–1,011.^{40,44,47,48,58,60,62,71,76}

Unfortunately, none of the studies quantitatively reported the circulation kinetics of the curcumin nanocarrier and thus no firm conclusions can be drawn regarding the PK of curcumin versus its carrier system. Further research is therefore needed to understand particle stability in the circulation and in relation to the PK of nanoencapsulated curcumin. Above all, it is recommended to covalently attach the fluorescent dye to the nanocarrier because loaded dyes can be released or extracted from the carrier system and thwart data interpretation due to differential PK and disposition compared to the nano carrier.¹¹²

4. IMPROVED AUC DOES NOT NECESSARILY TRANSLATE TO IMPROVED THERAPEUTIC EFFICACY

The main challenges that have been addressed above pertain to curcumin PK and center on curcumin retention in the circulation. It was concluded that certain nanoformulations are capable of improving the otherwise grim PK profile of curcumin following intravenous delivery. As blood vessels constitute the main conduit for a drug to reach a tumor, rapid exit of a drug from the bloodstream into tissues is detrimental to therapeutic efficacy. Given the poor retention of free curcumin in the circulation, intravenous administration of free curcumin is unlikely a viable approach to systemic therapy. Nanoformulations with stealth-like properties and effective tumor targeting are therefore the only potentially fruitful intervention strategy. The optimized PK associated with the nanoformulations under investigation does not by definition translate to (improved) PD efficacy. We therefore examined whether a correlation exists between PK and PD of free curcumin and curcumin nanoformulations using published studies that employed murine models of cancer. It was hypothesized that free curcumin would induce some TGI compared to vehicle control and that the antitumor activity would be exacerbated by nanoencapsulation. Moreover, it was expected that an increasing AUC, injected dose, and NC:C AUC ratio would (1) lead to higher antitumor activity (i.e., an increasing nominal difference in %TGI) and (2) widen the difference in %TGI between free versus nanoformulated curcumin.

The studies that met the inclusion criteria are summarized in Table 3. In a case-matched analysis, the animals that received curcumin nanoformulations exhibited more profound therapeutic effects than those that received free curcumin, which is in line with the increased AUC due to nanoencapsulation. Curcumin is cytostatic and cytotoxic to cancer cells⁶ but also interferes with other important features of tumor biology such as angiogenesis,^{57,58,60,71,76} which theoretically should lead to greater PD with improved PK. It must be noted that, in some studies,^{46,47,57,58,60,61,76,77} the PK parameters were reported in wild-type rats, while the therapeutic efficacy was determined in tumor-bearing immunocompromised mice.

To systematically assess the relationship between PK and PD in a clustered analysis, the nominal difference in %TGI achieved with free curcumin and curcumin nanoformulations (compared to respective controls) was plotted versus AUC, total injected dose, and the NC:C AUC ratio (Figure 7A–C) to derive Spearman's correlation coefficient. These analyses give insight into the validity of the putative premises that (AUC \uparrow \rightarrow PD \uparrow) and (systemic concentration \uparrow \rightarrow PD \uparrow).

In terms of AUC, an increase in therapeutic efficacy (difference in %TGI) at higher AUCs was not observed

when nanoformulated curcumin (NC) was compared to vehicle/solvent control, as evidenced by the lack of positive correlation (Figure 7A, red data points and statistics table below). The same applies to free curcumin (C), which further exhibited a generally lower AUC and nominal difference in %TGI compared to solvent control than the nanoformulated curcumin group (Figure 7A, blue data points). When NC was compared to C and plotted as a function of AUC (of NC), the therapeutic efficacy abated with improved PK of NC (Figure 7A, green data points) given the strong negative, albeit nonsignificant correlation. A clear explanation for this phenomenon is presently at large. It is possible that (1) there is a nonlinear relationship between circulation time and intratumoral NC delivery, (2) uptake of NC impedes cell death cascades compared to internalized C, (3) C accumulated in the tumor to a sufficient degree to induce cell death despite poor PK (during the distribution phase, especially in studies where micelle-forming surfactant molecules were used to solubilize free curcumin; see section 3.1), or (4) the NC did not extravasate from the blood vessels, hampering the delivery of cytotoxic cargo into the target cells. Other contributing factors may be the variety in the type of nanoformulations, tumor models, the discrepancy between PK/PD animal models, and/or different time frames that animals were monitored. Naturally, the eventual strength of the PK–PD correlation analysis relies on the translatability of curcumin PK in rats to the mouse situation, in which all the PD studies were conducted.

Comparable outcomes were observed when the difference in %TGI was plotted as a function of injected dose (Figure 7B). Administration of more NC or C did not yield more tumoricidal or cytostatic effects. Moreover, a strong and significant negative correlation was observed in the NC versus C comparison group when plotted as a function of injected dose (of NC). For this group, the dosages were matched. This finding is particularly striking in light of the fact that nanoencapsulation improves the measured C_{\max} (section 3.1) and the AUC (section 3.2) while decreasing the V_d and CL for some formulations (section 3.4). An increasing injected dosage on top of those inherently advantageous properties was therefore expected to exacerbate the %TGI of NC and its divergence from the %TGI of C.

In the final set of analyses, the NC:C AUC ratio was calculated and plotted versus the difference in %TGI. In this approach the effect on PD is considered from a quantitative improvement in the PK of NC, which is then compared to vehicle/solvent control (Figure 7C, red data points) or to C (Figure 7C, green data points) in terms of anticancer efficacy. With this analysis, the potential %TGI-amplifying effects of a protracted AUC of C (due to micelle-forming solvent molecules) was corrected. Nevertheless, the nanoformulations with a relatively low NC:C AUC ratio performed equally well if not better than the more stable nanoformulations^{57,58,61,70,71,77} with a relatively high NC:C AUC ratio, dismissing the notion that a prolonged curcumin circulation time and thus higher AUC leads to better treatment outcome.

Lastly, the same set of analyses was performed for one type of polymer formulation to eliminate PK–PD differences owing to the use of different types of materials. Copolymers of methoxy poly(ethylene glycol)-*block*-poly(ϵ -caprolactone) (mPEG-PCL) are frequently used for the solubilization and delivery of hydrophobic drugs,¹¹³ including curcumin (Table 3). The eligible studies^{60,70,71,76} encompassed mPEG-PCL

block copolymers with equal hydrophilic and hydrophobic molecular weights (2000 g/mol). The results are presented in Figure 7D–F.

The first notable observation from the data is that an injection dose range of only 300 mg/kg (200–500 mg/kg; Figure 7E) yielded an AUC spread of 3 orders of magnitude (Figure 7D) when assayed in the same animal species.^{60,76} Differences in the experimental and analytical techniques used might explain this discrepancy, which pleads for protocol standardization to enable interstudy comparisons. Second, a higher AUC (Figure 7D) or injected dose (Figure 7E) did not lead to improved therapeutic efficacy and generated contrasting data. Gong et al.⁷¹ and Gou et al.⁶⁰ reported around 50% tumor reduction compared to the untreated group after administration of 25 mg/kg curcumin-loaded mPEG-PCL micelles every 2 days for 2 weeks in mice bearing LL/2 Lewis lung carcinoma and 25 mg/kg daily for 10 days in mice bearing C26 murine colon carcinoma tumor xenografts, respectively. Contrastingly, curcumin-loaded mPEG-PCL micelles did not exhibit tumor reduction compared to the control group (physiological saline) in mice bearing K567/ADR chronic myelogenous leukemia xenografts following a curcumin dosing schedule of 40 mg/kg every day for 3 weeks. This could be due to the similar PK of curcumin-loaded mPEG-PCL and free curcumin reported in this study (no difference in AUC was observed) and/or attributable to the multidrug resistance phenotype of K562/ADR cells. The *N*-(*tert*-butoxycarbonyl)-*L*-phenylalanine end-capped mPEG-PCL micelles with higher stability yielded a 65% tumor reduction compared to the untreated group.⁷⁰ Third, despite uniformity in drug delivery systems, the AUC ratio of mPEG-PCL micelles to free curcumin was different among the studies. Gong et al.,⁷¹ Gou et al.⁶⁰ and Hu et al.⁷⁶ reported AUC ratios of 5.0, 6.0, and 7.7, respectively, whereas Gong et al. found an AUC ratio of 1.1.⁷⁰ There was no evident positive correlation between PK and PD, altogether attesting to the main conclusion that, although nanoformulations improve curcumin PK (AUC), this does not as a rule result in greater oncotherapeutic efficacy.

5. PRELIMINARY TRANSLATIONAL AND CLINICAL OUTCOMES OF INTRAVENOUS CURCUMIN NANOFORMULATIONS

Presently there are only two intravenous curcumin nanoformulations (Lipocurc and CUC-01) registered in the clinicaltrials.gov database for cancer treatment. To date, the efficacy and safety of CUC-01, a curcuminoid formulation in polyoxyl castor oil (Kolliphor ELP) as a nonionic solubilizer, was evaluated in patients with metastatic breast cancer in combination with paclitaxel following intravenous administration of both. As explained earlier, using such surfactants as solubilizers results in micellar nanoformulations. The authors reported that the combination therapy was superior to paclitaxel plus placebo without major safety concerns.¹¹⁴

The PK and biodistribution profile of Lipocurc, a liposomal curcumin formulation, have been extensively investigated in dogs and humans in several studies. The impact of the duration of intravenous infusion of Lipocurc on curcumin metabolism and tissue distribution was assessed in dogs. The tissue levels of curcumin and its metabolite tetrahydrocurcumin in the lungs, spleen, and liver were substantially higher after the 8-h regimen compared to the 2-h regimen. Also, the longer infusion time resulted in a higher tissue partition coefficient for curcumin and tetrahydrocurcumin. The ratio of the metabolite

to curcumin was lower during longer infusion regimens and different in a tissue-specific manner. The authors argued that the extended infusion might facilitate the distribution of curcumin into tissues by a transporter-dependent mechanism and that higher tissue concentrations of curcumin might inhibit or saturate a putative reductase enzyme that converts curcumin to its metabolite.¹¹⁵ However, later the authors suggested another mechanism to substantiate these observations by performing complementary *in vitro* experiments that are discussed below.^{81,116,117}

The pharmacokinetic profile, safety, and tolerability of Lipocurc were studied in a phase I dose escalation trial following a single bolus intravenous injection in the range of 10–400 mg/m². The plasma concentration of curcumin and tetrahydrocurcumin increased in a dose-dependent manner. Shortly after discontinuation of the infusion (6–60 min), the curcumin concentration in plasma fell below the detection limit. Intravenous dosing was safe and above 120 mg/m² a transient change in the morphology of red blood cells (RBCs) was noticed. Therefore, short-term infusion of Lipocurc was deemed safe up to 120 mg/m², and higher doses represented dose-limiting toxicity in RBCs.¹¹⁶ In subsequent experiments the authors confirmed *in vitro* that curcumin and liposomal curcumin caused morphological changes in RBCs in a dose-dependent manner.¹¹⁷

In the wake of these observations, the cellular distribution and metabolism of curcumin (formulated as Lipocure) were investigated *in vitro* in RBCs and peripheral blood mononuclear cells (PBMCs). It was demonstrated that curcumin rapidly distributed into RBCs and PBMCs. The authors assumed that Lipocurc adsorbs onto the cell membrane of RBC/PBMCs, after which curcumin diffuses across the cell membrane into the intracellular compartment. Blood-based metabolism, in particular in RBCs, was observed as 92% and 68% of curcumin disappeared from the medium as soon as 15 min after the addition of canine and human RBCs, respectively. Thus, incorporation of curcumin and subsequent metabolism into tetrahydrocurcumin and possibly other metabolites occurs in human and canine RBCs. Although the type of enzyme(s) responsible for the metabolism is not yet clear, the authors proposed an enzyme comparable to dihydrocurcumin reductase in gut microorganisms or cytochrome b5 reductase that is present in mammalian cells, including RBCs.¹¹⁸

The findings are relevant for the PK profile of curcumin. Together with organ-based metabolism and possibly chemical instability, the data explain why steady-state levels of curcumin were not achieved after infusion and provide a rationale for the short plasma half-lives. The authors hypothesized that RBCs might serve as a vehicle to distribute curcumin to tissues due to the cell's fractional abundance in blood. This, according to the authors, may explain the higher curcumin concentration in tissues after eight-hour infusion compared to two-hour infusion. When reported in terms of per cell basis, curcumin was retrieved at a higher concentration in PBMCs compared to RBCs, which can be of potential therapeutic utility in the treatment of tumors with lymphocytic origin.⁸¹ Following up on this observation, the authors demonstrated higher curcumin distribution into PBMCs in chronic lymphocytic leukemia patient-derived PBMCs compared to healthy donors¹¹⁹ and higher uptake in multiple myeloma cell lines,¹²⁰ underpinning a potential therapeutic benefit in the treatment of hematological cancers. Therefore, the role of RBCs in the PK and PD of curcumin should be evaluated carefully. Apart from being an

intrinsic carrier, accumulation and subsequent metabolism of curcumin may yield less active metabolites that are ready to be cleared.

6. CONCLUSIONS AND OUTLOOK

Curcumin is a compound with PD potency but PK frailty, characterized by rapid removal from plasma during the distribution phase and the absence of steady-state plasma levels after intravenous administration. Consequently, curcumin's PD potency does not come to fruition *in vivo*. Our systematic analysis of animal studies revealed that curcumin loading into nanocarriers is beneficial for the compound's PK profile in that nanoencapsulation improved the measured C_{\max} and AUC while reducing the V_d and CL compared to the free form. However, these effects were not ubiquitous and depended on the nanoformulation type. Also, certain curcumin nanoformulations were associated with a greater %TGI compared to free curcumin in different tumor models, which is in line with the improved PK profile. However, clustered analysis revealed that there is no positive correlation between AUC as well as injected dose and antitumor efficacy. In addition, almost all studies neglected to investigate the nanocarrier's PK profile and ability to deliver cargo into the target cells. Those few papers that followed up on the circulation kinetics of the nanocarrier did not report the data quantitatively. Therefore, at this point, it is not possible to firmly conclude whether stable nanoformulations with high curcumin retention are required for better therapeutic efficacy than nanoformulations that are merely solubilizers. It is therefore recommended that future investigations on curcumin nanoformulations as oncotherapeutics go beyond the classical PK parameters and focus mainly on intratumoral curcumin levels as a function of time after administration and corollary effects on tumor volume or mass. Based on our analysis, the classical PK parameters are inadequate and cannot be employed as barometers for therapeutic efficacy, rendering studies that focus solely on the PK of curcumin nanoformulations equally inadequate in broader context.

The rapid distribution of curcumin into blood cells leads to compartmentalization that could skew conclusions regarding curcumin bioavailability (in case of oral formulations) and circulation time. Whole blood-based assays should be developed and used to quantitate curcumin levels in blood. It is also possible that curcumin exploits blood cells as temporary carriers and eventually redistributes from the cellular compartment to plasma or is trafficked into the tumor microenvironment via a cellular carrier. Acquiring a more thorough understanding of these phenomena will spawn higher-resolution insight into curcumin's PK–PD relationship in terms of solid malignancies. Further room for improvement lies in optimizing administration regimens, where injection over a longer period of time has shown promise in dogs in regard to more profound tissue accumulation.¹¹⁵ For hematological malignancies, on the other hand, the blood cell-occupying behavior of curcumin may de facto be conducive to treatment efficacy.

■ ASSOCIATED CONTENT

SI Supporting Information

The Supporting Information is available free of charge at <https://pubs.acs.org/doi/10.1021/acs.molpharmaceut.2c00455>.

Details regarding pharmacokinetics principles and calculation methods, tables containing raw data of PK parameters extracted from literature, and comparison between calculated and measured AUC values *in vivo* for free curcumin and curcumin nanoformulations (PDF)

■ AUTHOR INFORMATION

Corresponding Author

Michal Heger – Department of Pharmaceutics, Utrecht Institute for Pharmaceutical Sciences, Utrecht University, 3584 CG Utrecht, The Netherlands; Jiaxing Key Laboratory for Photonanomedicine and Experimental Therapeutics, Department of Pharmaceutics, College of Medicine, Jiaxing University, Jiaxing, Zhejiang 314001, PR China; orcid.org/0000-0002-0630-4465; Phone: +31-6-24483083; Email: m.heger@uu.nl, m.heger@jctres.com

Authors

Mahsa Bagheri – Department of Pharmaceutics, Utrecht Institute for Pharmaceutical Sciences, Utrecht University, 3584 CG Utrecht, The Netherlands

Cornelius F. van Nostrum – Department of Pharmaceutics, Utrecht Institute for Pharmaceutical Sciences, Utrecht University, 3584 CG Utrecht, The Netherlands; orcid.org/0000-0003-4210-5241

Robbert Jan Kok – Department of Pharmaceutics, Utrecht Institute for Pharmaceutical Sciences, Utrecht University, 3584 CG Utrecht, The Netherlands; orcid.org/0000-0003-4933-3968

Gert Storm – Department of Pharmaceutics, Utrecht Institute for Pharmaceutical Sciences, Utrecht University, 3584 CG Utrecht, The Netherlands

Wim E. Hennink – Department of Pharmaceutics, Utrecht Institute for Pharmaceutical Sciences, Utrecht University, 3584 CG Utrecht, The Netherlands; orcid.org/0000-0002-5750-714X

Complete contact information is available at:

<https://pubs.acs.org/10.1021/acs.molpharmaceut.2c00455>

Author Contributions

Conceptualization: M.B., W.E.H., and M.H.; funding acquisition: W.E.H. and M.H.; data curation and formal analysis: M.B. and M.H.; writing - original draft: M.B. and M.H.; writing - review and editing: M.H., W.E.H., R.J.K., C.F.v.N., and G.S.; supervision: M.H. and W.E.H. All authors have read and agreed to the published version of the manuscript and assume responsibility for its entire content.

Funding

This project was supported by the European Union's Horizon 2020 research and innovation program Marie Skłodowska-Curie Innovative Training Networks (ITN) under grant no. 676137. M. Heger was supported by grants from the Dutch Cancer Foundation (KWF project no. 10666), a Zhejiang Provincial Foreign Expert Program Grant, Zhejiang Provincial Key Natural Science Foundation of China (no. Z20H160031), and a grant for the establishment of the Jiaxing Key Laboratory for Photonanomedicine and Experimental Therapeutics.

Notes

The authors declare the following competing financial interest(s): Michal Heger is chief formulation officer at Camelina Sun LLC. There are no other conflicts of interest.

■ ABBREVIATIONS

AUC, area under the curve; PK, pharmacokinetics; PD, pharmacodynamic; TGI, tumor growth inhibition; S, Supporting Information; C_{\max} , maximum concentration; $t_{1/2}$, elimination half-life; CL, clearance; V_d , distribution volume; CN, curcumin nanoformulation; C, free curcumin; PBS, phosphate buffered saline; RBC, red blood cell; HA, hyaluronic acid; ZP, ζ potential; ID, injected dose; DMSO, dimethyl sulfoxide; PEG, polyethylene glycol; d, days; NA, not available; SD, Sprague–Dawley; s.c., subcutaneous; i.v., intravenous; CTRL, control; PBMCS, peripheral blood mononuclear cells; HA-curc-NC, hyaluronic acid-coated curcumin nanocrystals; mPEG-PLGA, (polyethylene glycol)-poly(lactic-co-glycolic acid); mPEG-b-PHEMA-SHA micelles, pH-responsive reversibly cross-linked micelles poly(ethylene glycol)-*b*-poly(2-methacrylate ethyl 5-hexynoate); zein-PSBMA micelles, zein-poly(sulfobetaine methacrylate); HA-Cur-LPs, hyaluronic acid modified liposomes; (PDLLA-G)-based nanoparticles, poly(D,L-lactic acid)-glycerol-based nanoparticles; curcumin-PBCA nanoparticles, cationic poly(butyl) cyanoacrylate nanoparticles coated with chitosan; mPEG-PLA, monomethoxy poly(ethylene glycol)poly(lactide); mPEG-PCL-Phe(Boc) micelles, methoxy-poly(ethyleneglycol)-*block*-poly(ϵ -caprolactone) and *N*-(*tert*-butoxycarbonyl)-L-phenylalanine end-capped; mPEG-PCL, methoxy poly(ethylene glycol)-*block*-poly(ϵ -caprolactone); mPEG-PLA-PAE, pH-sensitive methoxy poly(ethylene glycol)-poly(lactide)-poly(β -amino ester); mPEG-b-PHEMA-SHA, pH-responsive reversibly cross-linked micelles poly(ethylene glycol)-*b*-poly(2-methacrylate ethyl 5-hexynoate); HA-curc-NC, hyaluronic acid-modified curcumin nanocrystals; mPEG-DSPE, monomethoxy poly(ethylene glycol)-distearoyl phosphatidylcholine; SPC, soybean lecithin; HSA, human serum albumin

■ REFERENCES

- (1) Sharma, R. A.; Gescher, A. J.; Steward, W. P. Curcumin: The story so far. *Eur. J. Cancer* **2005**, *41*, 1955–1968.
- (2) Kotha, R. R.; Luthria, D. L. Curcumin: Biological, pharmaceutical, nutraceutical, and analytical aspects. *Molecules* **2019**, *24*, 2930.
- (3) Doello, K.; Ortiz, R.; Alvarez, P. J.; Melguizo, C.; Cabeza, L.; Prados, J. Latest in vitro and in vivo assay, clinical trials and patents in cancer treatment using curcumin: A literature review. *Nutr. Cancer* **2018**, *70*, 569–578.
- (4) Patel, S. S.; Acharya, A.; Ray, R. S.; Agrawal, R.; Raghuwanshi, R.; Jain, P. Cellular and molecular mechanisms of curcumin in prevention and treatment of disease. *Crit. Rev. Food Sci. Nutr.* **2020**, *60*, 887–939.
- (5) Shehzad, A.; Wahid, F.; Lee, Y. S. Curcumin in cancer chemoprevention: Molecular targets, pharmacokinetics, bioavailability, and clinical trials. *Arch. Pharm.* **2010**, *343*, 489–499.
- (6) Heger, M.; van Golen, R. F.; Broekgaarden, M.; Michel, M. C. The molecular basis for the pharmacokinetics and pharmacodynamics of curcumin and its metabolites in relation to cancer. *Pharmacol. Rev.* **2014**, *66*, 222–307.
- (7) Heger, M. Drug screening: Don't discount all curcumin trial data. *Nature* **2017**, *543*, 40.
- (8) Balaji, S.; Chempakam, B. Toxicity prediction of compounds from turmeric (*Curcuma longa* L.). *Food Chem. Toxicol.* **2010**, *48*, 2951–2959.
- (9) Cheng, A. L.; Hsu, C. H.; Lin, J. K.; Hsu, M. M.; Ho, Y. F.; Shen, T. S.; Ko, J. Y.; Lin, J. T.; Lin, B. R.; Ming-Shiang, W.; Yu, H. S.; Jee, S. H.; Chen, G. S.; Chen, T. M.; Chen, C. A.; Lai, M. K.; Pu, Y. S.; Pan, M. H.; Wang, Y. J.; Tsai, C. C.; Hsieh, C. Y. Phase I clinical trial of curcumin, a chemopreventive agent, in patients with high-risk or pre-malignant lesions. *Anticancer Res.* **2001**, *21*, 2895–2900.
- (10) Yeung, A. W. K.; Horbańczuk, M.; Tzvetkov, N. T.; Mocan, A.; Carradori, S.; Maggi, F.; Marchewka, J.; Sut, S.; Dall'Acqua, S.; Gan, R.-Y.; Tancheva, L. P.; Polgar, T.; Berindan-Neagoe, I.; Pirgozliev, V.; Šmejkal, K.; Atanasov, A. G. Curcumin: Total-scale analysis of the scientific literature. *Molecules* **2019**, *24*, 1393.
- (11) Willenbacher, E.; Khan, S. Z.; Mujica, S. C. A.; Trapani, D.; Hussain, S.; Wolf, D.; Willenbacher, W.; Spizzo, G.; Seeber, A. Curcumin: New insights into an ancient ingredient against cancer. *Int. J. Mol. Sci.* **2019**, *20*, 1808.
- (12) Duvoix, A.; Blasius, R.; Delhalle, S.; Schneckeburger, M.; Morceau, F.; Henry, E.; Dicato, M.; Diederich, M. Chemopreventive and therapeutic effects of curcumin. *Cancer Lett.* **2005**, *223*, 181–190.
- (13) Shanmugam, M. K.; Rane, G.; Kanchi, M. M.; Arfuso, F.; Chinnathambi, A.; Zayed, M. E.; Alharbi, S. A.; Tan, B. K.; Kumar, A. P.; Sethi, G. The multifaceted role of curcumin in cancer prevention and treatment. *Molecules* **2015**, *20*, 2728–2769.
- (14) Ismail, N.I.; Othman, I.; Abas, F.; Lajis, N. H.; Naidu, R. Mechanism of apoptosis induced by curcumin in colorectal cancer. *Int. J. Mol. Sci.* **2019**, *20*, 2454.
- (15) Giordano, A.; Tommonaro, G. Curcumin and cancer. *Nutrients* **2019**, *11*, 2376.
- (16) Ravindran, J.; Prasad, S.; Aggarwal, B. B. Curcumin and cancer cells: How many ways can curry kill tumor cells selectively? *AAPS J.* **2009**, *11*, 495–510.
- (17) Syng-Ai, C.; Kumari, A. L.; Khar, A. Effect of curcumin on normal and tumor cells: role of glutathione and bcl-2. *Molecular cancer therapeutics* **2004**, *3*, 1101–1108.
- (18) Chang, R.; Sun, L.; Webster, T. J. Short communication: selective cytotoxicity of curcumin on osteosarcoma cells compared to healthy osteoblasts. *Int. J. Nanomed.* **2014**, *9*, 461–465.
- (19) Mehta, H. J.; Patel, V.; Sadikot, R. T. Curcumin and lung cancer—a review. *Target Oncol.* **2014**, *9*, 295–310.
- (20) Bimonte, S.; Barbieri, A.; Leongito, M.; Piccirillo, M.; Giudice, A.; Pivonello, C.; de Angelis, C.; Granata, V.; Palaia, R.; Izzo, F. Curcumin antiCancer studies in pancreatic cancer. *Nutrients* **2016**, *8*, 433.
- (21) Shureiqi, I.; Baron, J. A. Curcumin chemoprevention: The long road to clinical translation. *Cancer Prev. Res.* **2011**, *4*, 296.
- (22) Dhillion, N.; Aggarwal, B. B.; Newman, R. A.; Wolff, R. A.; Kunnumakkara, A. B.; Abbruzzese, J. L.; Ng, C. S.; Badmaev, V.; Kurzrock, R. Phase II trial of curcumin in patients with advanced pancreatic cancer. *Clin. Cancer Res.* **2008**, *14*, 4491.
- (23) Mohamed, S. A.; El-Shishtawy, R. M.; Al-Bar, O. A. M.; Al-Najada, A. R. Chemical modification of curcumin: Solubility and antioxidant capacity. *Int. J. Food Prop.* **2017**, *20*, 718–724.
- (24) Subramaniam, D.; May, R.; Sureban, S. M.; Lee, K. B.; George, R.; Kuppusamy, P.; Ramanujam, R. P.; Hideg, K.; Dieckgraefe, B. K.; Houchen, C. W.; Anant, S. Diphenyl difluoroketone: A curcumin derivative with potent in vivo anticancer activity. *Cancer Res.* **2008**, *68*, 1962.
- (25) Li, Q.; Zhai, W.; Jiang, Q.; Huang, R.; Liu, L.; Dai, J.; Gong, W.; Du, S.; Wu, Q. Curcumin–piperine mixtures in self-micro-emulsifying drug delivery system for ulcerative colitis therapy. *Int. J. Pharm.* **2015**, *490*, 22–31.
- (26) Shoba, G.; Joy, D.; Joseph, T.; Majeed, M.; Rajendran, R.; Srinivas, P. S. S. R. Influence of piperine on the pharmacokinetics of cCurcumin in animals and human volunteers. *Planta Med.* **1998**, *64*, 353–356.
- (27) Mirzaei, H.; Shakeri, A.; Rashidi, B.; Jalili, A.; Banikazemi, Z.; Sahebkar, A. Phytosomal curcumin: A review of pharmacokinetic, experimental and clinical studies. *Biomed. Pharmacother.* **2017**, *85*, 102–112.
- (28) Naksuriya, O.; Okonogi, S.; Schiffelers, R. M.; Hennink, W. E. Curcumin nanoformulations: A review of pharmaceutical properties and preclinical studies and clinical data related to cancer treatment. *Biomaterials* **2014**, *35*, 3365–3383.

- (29) Yallapu, M. M.; Jaggi, M.; Chauhan, S. C. Curcumin nanoformulations: a future nanomedicine for cancer. *Drug discovery today* **2012**, *17*, 71–80.
- (30) Mohanty, C.; Das, M.; Sahoo, S. K. Emerging role of nanocarriers to increase the solubility and bioavailability of curcumin. *Expert opinion on drug delivery* **2012**, *9*, 1347–1364.
- (31) Khezri, K.; Saeedi, M.; Mohammadamini, H.; Zakaryaei, A.S. A comprehensive review of the therapeutic potential of curcumin nanoformulations. *Phytotherapy Research* **2021**, *35*, 5527–5563.
- (32) Patra, J. K.; Das, G.; Fraceto, L. F.; Campos, E. V. R.; Rodriguez-Torres, M.d.P.; Acosta-Torres, L. S.; Diaz-Torres, L. A.; Grillo, R.; Swamy, M. K.; Sharma, S.; Habtemariam, S.; Shin, H.-S. Nano based drug delivery systems: recent developments and future prospects. *J. Nanobiotechnol.* **2018**, *16*, 71.
- (33) Mirza, A. Z.; Siddiqui, F. A. Nanomedicine and drug delivery: a mini review. *Int. Nano Lett.* **2014**, *4*, 94.
- (34) Varela-Moreira, A.; Shi, Y.; Fens, M. H. A. M.; Lammers, T.; Hennink, W. E.; Schiffelers, R. M. Clinical application of polymeric micelles for the treatment of cancer. *Mater. Chem. Front.* **2017**, *1*, 1485–1501.
- (35) Deng, C.; Jiang, Y.; Cheng, R.; Meng, F.; Zhong, Z. Biodegradable polymeric micelles for targeted and controlled anticancer drug delivery: Promises, progress and prospects. *Nano Today* **2012**, *7*, 467–480.
- (36) Bobo, D.; Robinson, K. J.; Islam, J.; Thurecht, K. J.; Corrie, S. R. Nanoparticle-based medicines: a review of FDA-approved materials and clinical trials to date. *Pharm. Res.* **2016**, *33*, 2373–2387.
- (37) Naksuriya, O.; van Steenberg, M. J.; Torano, J. S.; Okonogi, S.; Hennink, W. E. A kinetic degradation study of curcumin in its free form and loaded in polymeric micelles. *AAPS J.* **2016**, *18*, 777–787.
- (38) Anselmo, A. C.; Mitragotri, S. Nanoparticles in the clinic: An update. *Bioengineering & Translational Medicine* **2019**, *4*, No. e10143.
- (39) Zhong, H.; Chan, G.; Hu, Y.; Hu, H.; Ouyang, D. A Comprehensive Map of FDA-Approved Pharmaceutical Products. *Pharmaceutics* **2018**, *10*, 263.
- (40) Sun, D.; Zhou, J.-K.; Zhao, L.; Zheng, Z.-Y.; Li, J.; Pu, W.; Liu, S.; Liu, X.-S.; Liu, S.-J.; Zheng, Y.; Zhao, Y.; Peng, Y. Novel curcumin liposome modified with hyaluronan targeting CD44 plays an anti-leukemic role in acute myeloid leukemia in vitro and in vivo. *ACS Appl. Mater. Interfaces* **2017**, *9*, 16857–16868.
- (41) Yu, Y.; Zhang, X.; Qiu, L. The anti-tumor efficacy of curcumin when delivered by size/charge-changing multistage polymeric micelles based on amphiphilic poly(beta-amino ester) derivatives. *Biomaterials* **2014**, *35*, 3467–3479.
- (42) Zou, P.; Helson, L.; Maitra, A.; Stern, S. T.; McNeil, S. E. Polymeric curcumin nanoparticle pharmacokinetics and metabolism in bile duct cannulated rats. *Mol. Pharmaceutics* **2013**, *10*, 1977–1987.
- (43) Duan, D.; Wang, A.; Ni, L.; Zhang, L.; Yan, X.; Jiang, Y.; Mu, H.; Wu, Z.; Sun, K.; Li, Y. Trastuzumab- and Fab' fragment-modified curcumin PEG-PLGA nanoparticles: preparation and evaluation in vitro and in vivo. *Int. J. Nanomed.* **2018**, *13*, 1831–1840.
- (44) Wu, W.; Wu, J.; Fu, Q.; Jin, C.; Guo, F.; Yan, Q.; Yang, Q.; Wu, D.; Yang, Y.; Yang, G. Elaboration and characterization of curcumin-loaded Tri-CL-mPEG three-arm copolymeric nanoparticles by a microchannel technology. *Int. J. Nanomed.* **2019**, *14*, 4683–4695.
- (45) Lollo, G.; Ullio-Gamboa, G.; Fuentes, E.; Matha, K.; Lautram, N.; Benoit, J.-P. In vitro anti-cancer activity and pharmacokinetic evaluation of curcumin-loaded lipid nanocapsules. *Mater. Sci. Eng., C* **2018**, *91*, 859–867.
- (46) Liu, Y.; Chen, F.; Zhang, K.; Wang, Q.; Chen, Y.; Luo, X. pH-Responsive reversibly cross-linked micelles by phenol–yne click via curcumin as a drug delivery system in cancer chemotherapy. *J. Mater. Chem. B* **2019**, *7*, 3884–3893.
- (47) Ji, P.; Wang, L.; Chen, Y. W.; Wang, S. Q.; Wu, Z. H.; Qi, X. L. Hyaluronic acid hydrophilic surface rehabilitating curcumin nanocrystals for targeted breast cancer treatment with prolonged biodistribution. *Biomater. Sci.* **2020**, *8*, 462–472.
- (48) Yoon, I.-S.; Park, J.-H.; Kang, H. J.; Choe, J. H.; Goh, M. S.; Kim, D.-D.; Cho, H.-J. Poly(D,L-lactic acid)-glycerol-based nanoparticles for curcumin delivery. *Int. J. Pharm.* **2015**, *488*, 70–77.
- (49) Wu, Z.; Cai, M.; Xie, X.; He, L.; Huang, L.; Chen, Y.; Luo, X. The effect of architecture/composition on the pH sensitive micelle properties and in vivo study of curcumin-loaded micelles containing sulfobetaines. *RSC Adv.* **2015**, *5*, 106989–107000.
- (50) Sun, J.; Bi, C.; Chan, H. M.; Sun, S.; Zhang, Q.; Zheng, Y. Curcumin-loaded solid lipid nanoparticles have prolonged in vitro antitumor activity, cellular uptake and improved in vivo bioavailability. *Colloids Surf., B* **2013**, *111*, 367–375.
- (51) Xu, Y.; Asghar, S.; Yang, L.; Chen, Z.; Li, H.; Shi, W.; Li, Y.; Shi, Q.; Ping, Q.; Xiao, Y. Nanoparticles based on chitosan hydrochloride/hyaluronic acid/PEG containing curcumin: In vitro evaluation and pharmacokinetics in rats. *Int. J. Biol. Macromol.* **2017**, *102*, 1083–1091.
- (52) Zhai, S.; Ma, Y.; Chen, Y.; Li, D.; Cao, J.; Liu, Y.; Cai, M.; Xie, X.; Chen, Y.; Luo, X. Synthesis of an amphiphilic block copolymer containing zwitterionic sulfobetaine as a novel pH-sensitive drug carrier. *Polym. Chem.* **2014**, *5*, 1285–1297.
- (53) Chen, S.; Li, Q.; Li, H.; Yang, L.; Yi, J.-Z.; Xie, M.; Zhang, L.-M. Long-circulating zein-polysulfobetaine conjugate-based nanocarriers for enhancing the stability and pharmacokinetics of curcumin. *Mater. Sci. Eng., C* **2020**, *109*, 110636.
- (54) Chen, D.; Sun, J. In vitro and in vivo evaluation of PEG-conjugated ketal-based chitosan micelles as pH-sensitive carriers. *Polym. Chem.* **2015**, *6*, 998–1004.
- (55) Bagheri, M.; Fens, M. H.; Kleijn, T. G.; Capomaccio, R. B.; Mehn, D.; Krawczyk, P. M.; Scutigliani, E. M.; Gurinov, A.; Baldus, M.; van Kronenburg, N. C. H.; Kok, R. J.; Heger, M.; van Nostrum, C. F.; Hennink, W. E. In Vitro and In Vivo Studies on HPMa-Based Polymeric Micelles Loaded with Curcumin. *Mol. Pharmaceutics* **2021**, *18*, 1247–1263.
- (56) Song, Z.; Feng, R.; Sun, M.; Guo, C.; Gao, Y.; Li, L.; Zhai, G. Curcumin-loaded PLGA-PEG-PLGA triblock copolymeric micelles: Preparation, pharmacokinetics and distribution in vivo. *J. Colloid Interface Sci.* **2011**, *354*, 116–123.
- (57) Duan, J.; Zhang, Y.; Han, S.; Chen, Y.; Li, B.; Liao, M.; Chen, W.; Deng, X.; Zhao, J.; Huang, B. Synthesis and in vitro/in vivo anti-cancer evaluation of curcumin-loaded chitosan/poly(butyl cyanoacrylate) nanoparticles. *Int. J. Pharm.* **2010**, *400*, 211–220.
- (58) Gao, X.; Zheng, F.; Guo, G.; Liu, X.; Fan, R.; Qian, Z.-y.; Huang, N.; Wei, Y.-q. Improving the anti-colon cancer activity of curcumin with biodegradable nano-micelles. *J. Mater. Chem. B* **2013**, *1*, 5778–5790.
- (59) Sun, M.; Gao, Y.; Guo, C.; Cao, F.; Song, Z.; Xi, Y.; Yu, A.; Li, A.; Zhai, G. Enhancement of transport of curcumin to brain in mice by poly(n-butylcyanoacrylate) nanoparticle. *J. Nanopart. Res.* **2010**, *12*, 3111–3122.
- (60) Gou, M.; Men, K.; Shi, H.; Xiang, M.; Zhang, J.; Song, J.; Long, J.; Wan, Y.; Luo, F.; Zhao, X.; Qian, Z. Curcumin-loaded biodegradable polymeric micelles for colon cancer therapy in vitro and in vivo. *Nanoscale* **2011**, *3*, 1558–1567.
- (61) Hong, J. Y.; Liu, Y. Y.; Xiao, Y.; Yang, X. F.; Su, W. J.; Zhang, M. Z.; Liao, Y. H.; Kuang, H. X.; Wang, X. T. High drug payload curcumin nanosuspensions stabilized by mPEG-DSPE and SPC: in vitro and in vivo evaluation. *Drug Delivery* **2017**, *24*, 109–120.
- (62) Yang, C.; Chen, H.; Zhao, J.; Pang, X.; Xi, Y.; Zhai, G. Development of a folate-modified curcumin loaded micelle delivery system for cancer targeting. *Colloids Surf., B* **2014**, *121*, 206–213.
- (63) Song, Z.; Zhu, W.; Yang, F.; Liu, N.; Feng, R. Preparation, characterization, in vitro release, and pharmacokinetic studies of curcumin-loaded mPEG-PVL nanoparticles. *Polym. Bull.* **2015**, *72*, 75–91.
- (64) Feng, R.; Song, Z.; Zhai, G. Preparation and in vivo pharmacokinetics of curcumin-loaded PCL-PEG-PCL triblock copolymeric nanoparticles. *Int. J. Nanomed.* **2012**, *7*, 4089–4098.
- (65) Smith, D. A.; Beaumont, K.; Maurer, T. S.; Di, L. Volume of distribution in drug design. *J. Med. Chem.* **2015**, *58*, 5691–5698.

- (66) Mansoor, A.; Mahabadi, N. Volume of distribution. In *StatPearls*; StatPearls Publishing, LLC, Treasure Island, FL, 2020.
- (67) Ravindranath, V.; Chandrasekhara, N. Absorption and tissue distribution of curcumin in rats. *Toxicology* **1980**, *16*, 259–265.
- (68) Ravindranath, V.; Chandrasekhara, N. Metabolism of curcumin-studies with [3H]curcumin. *Toxicology* **1981**, *22*, 337–344.
- (69) Holder, G. M.; Plummer, J. L.; Ryan, A. J. The metabolism and excretion of curcumin (1,7-bis-(4-hydroxy-3-methoxyphenyl)-1,6-heptadiene-3,5-dione) in the rat. *Xenobiotica; the fate of foreign compounds in biological systems* **1978**, *8*, 761–768.
- (70) Gong, F.; Chen, D.; Teng, X.; Ge, J.; Ning, X.; Shen, Y. L.; Li, J.; Wang, S. Curcumin-loaded blood-stable polymeric micelles for enhancing therapeutic effect on erythroleukemia. *Mol. Pharmaceutics* **2017**, *14*, 2585–2594.
- (71) Gong, C.; Deng, S.; Wu, Q.; Xiang, M.; Wei, X.; Li, L.; Gao, X.; Wang, B.; Sun, L.; Chen, Y.; Li, Y.; Liu, L.; Qian, Z.; Wei, Y. Improving antiangiogenesis and anti-tumor activity of curcumin by biodegradable polymeric micelles. *Biomaterials* **2013**, *34*, 1413–1432.
- (72) Song, Z.; Zhu, W.; Song, J.; Wei, P.; Yang, F.; Liu, N.; Feng, R. Linear-dendrimer type methoxy-poly (ethylene glycol)-b-poly (ϵ -caprolactone) copolymer micelles for the delivery of curcumin. *Drug Delivery* **2015**, *22*, 58–68.
- (73) Song, Z.; Zhu, W.; Liu, N.; Yang, F.; Feng, R. Linolenic acid-modified PEG-PCL micelles for curcumin delivery. *Int. J. Pharm.* **2014**, *471*, 312–321.
- (74) Jamwal, R. Bioavailable curcumin formulations: A review of pharmacokinetic studies in healthy volunteers. *J. Integr. Med.* **2018**, *16*, 367–374.
- (75) Nelson, K. M.; Dahlin, J. L.; Bisson, J.; Graham, J.; Pauli, G. F.; Walters, M. A. The Essential Medicinal Chemistry of Curcumin. *J. Med. Chem.* **2017**, *60*, 1620–1637.
- (76) Hu, Y. Z.; He, Y. H.; Ji, J. R.; Zheng, S. P.; Cheng, Y. Z. Tumor targeted curcumin delivery by folate-modified mPEG-PCL self-assembly micelles for colorectal cancer therapy. *Int. J. Nanomed.* **2020**, *15*, 1239–1252.
- (77) Song, Z.; Lu, Y.; Zhang, X.; Wang, H.; Han, J.; Dong, C. Novel curcumin-loaded human serum albumin nanoparticles surface functionalized with folate: characterization and in vitro/vivo evaluation. *Drug Des., Dev. Ther.* **2016**, *10*, 2643–2649.
- (78) Jiang, K.; Shen, M.; Xu, W. Arginine, glycine, aspartic acid peptide-modified paclitaxel and curcumin co-loaded liposome for the treatment of lung cancer: in vitro/vivo evaluation. *Int. J. Nanomed.* **2018**, *13*, 2561–2569.
- (79) Li, L.; Xiang, D.; Shigdar, S.; Yang, W.; Li, Q.; Lin, J.; Liu, K.; Duan, W. Epithelial cell adhesion molecule aptamer functionalized PLGA-lecithin-curcumin-PEG nanoparticles for targeted drug delivery to human colorectal adenocarcinoma cells. *Int. J. Nanomed.* **2014**, *9*, 1083–1096.
- (80) Ma, Z.; Shayeganpour, A.; Brocks, D. R.; Lavasanifar, A.; Samuel, J. High-performance liquid chromatography analysis of curcumin in rat plasma: application to pharmacokinetics of polymeric micellar formulation of curcumin. *Biomed. Chromatogr.* **2007**, *21*, 546–552.
- (81) Bolger, G. T.; Licollari, A.; Tan, A.; Greil, R.; Vcelar, B.; Majeed, M.; Helson, L. Distribution and metabolism of Lipocurc (liposomal curcumin) in dog and human blood cells: species selectivity and pharmacokinetic relevance. *Anticancer research* **2017**, *37*, 3483–3492.
- (82) Fujisawa, S.; Atsumi, T.; Ishihara, M.; Kadoma, Y. Cytotoxicity, ROS-generation activity and radical-scavenging activity of curcumin and related compounds. *Anticancer research* **2004**, *24*, 563–570.
- (83) Chen, G.; Chen, Y.; Yang, N.; Zhu, X.; Sun, L.; Li, G. Interaction between curcumin and mimetic biomembrane. *Sci. China Life Sci.* **2012**, *55*, 527–532.
- (84) Kopec, W.; Telenius, J.; Khandelia, H. Molecular dynamics simulations of the interactions of medicinal plant extracts and drugs with lipid bilayer membranes. *FEBS J.* **2013**, *280*, 2785–2805.
- (85) Ileri Ercan, N. Understanding Interactions of Curcumin with Lipid Bilayers: A Coarse-Grained Molecular Dynamics Study. *J. Chem. Inf. Model* **2019**, *59*, 4413–4426.
- (86) Wahlström, B.; Blennow, G. A study on the fate of curcumin in the rat. *Acta pharmacologica et toxicologica* **1978**, *43*, 86–92.
- (87) Gutiérrez-Gutiérrez, F.; Sánchez-Jiménez, C.; Rangel-Castañeda, I. A.; Carbajal-Arízaga, G. G.; Macías-Lamas, A. M.; Castillo-Romero, A.; Parra-Saavedra, K. J. Encapsulation of curcumin into layered double hydroxides improve their anticancer and antiparasitic activity. *J. Pharm. Pharmacol.* **2020**, *72*, 897–908.
- (88) Kolter, M.; Wittmann, M.; Köll-Weber, M.; Süß, R. The suitability of liposomes for the delivery of hydrophobic drugs – A case study with curcumin. *Eur. J. Pharm. Biopharm.* **2019**, *140*, 20–28.
- (89) Urso, R.; Bardi, P.; Giorgi, G. A short introduction to pharmacokinetics. *Eur. Rev. Med. Pharmacol. Sci.* **2002**, *6*, 33–44.
- (90) Schiborr, C.; Eckert, G. P.; Rimbach, G.; Frank, J. A validated method for the quantification of curcumin in plasma and brain tissue by fast narrow-bore high-performance liquid chromatography with fluorescence detection. *Anal. Bioanal. Chem.* **2010**, *397*, 1917–1925.
- (91) Lee, W. H.; Loo, C. Y.; Bebawy, M.; Luk, F.; Mason, R. S.; Rohanizadeh, R. Curcumin and its derivatives: their application in neuropharmacology and neuroscience in the 21st century. *Curr. Neuropharmacol* **2013**, *11*, 338–378.
- (92) Dempe, J. S.; Pfeiffer, E.; Grimm, A. S.; Metzler, M. Metabolism of curcumin and induction of mitotic catastrophe in human cancer cells. *Molecular nutrition & food research* **2008**, *52*, 1074–1081.
- (93) Jamil, Q. U. A.; Jaerapong, N.; Zehl, M.; Jarukamjorn, K.; Jäger, W. Metabolism of Curcumin in Human Breast Cancer Cells: Impact of Sulfation on Cytotoxicity. *Planta medica* **2017**, *83*, 1028–1034.
- (94) Removal of blood from laboratory mammals and birds. First report of the BVA/FRAME/RSPCA/UFOW Joint Working Group on Refinement. *Laboratory animals* **1993**, *27*, 1–22.
- (95) Sparreboom, A.; Scripture, C. D.; Trieu, V.; Williams, P. J.; De, T.; Yang, A.; Beals, B.; Figg, W. D.; Hawkins, M.; Desai, N. Comparative preclinical and clinical pharmacokinetics of a cremophor-free, nanoparticle albumin-bound paclitaxel (ABI-007) and paclitaxel formulated in Cremophor (Taxol). *Clin. Cancer Res.* **2005**, *11*, 4136–4143.
- (96) Kim, S. C.; Kim, D. W.; Shim, Y. H.; Bang, J. S.; Oh, H. S.; Kim, S. W.; Seo, M. H. In vivo evaluation of polymeric micellar paclitaxel formulation: toxicity and efficacy. *J. Controlled Release* **2001**, *72*, 191–202.
- (97) Youn, Y. S.; Bae, Y. H. Perspectives on the past, present, and future of cancer nanomedicine. *Adv. Drug Delivery Rev.* **2018**, *130*, 3–11.
- (98) Pan, M.-H.; Huang, T.-M.; Lin, J.-K. Biotransformation of Curcumin Through Reduction and Glucuronidation in Mice. *Drug Metab. Dispos.* **1999**, *27*, 486–494.
- (99) Felder-Flesch, D. *Dendrimers in nanomedicine*, 1st ed.; Jenny Stanford Publishing: New York, 2016.
- (100) Boussery, K.; Belpaire, F. M.; Van de Voorde, J. Physiological aspects determining the pharmacokinetic properties of drugs. In *The practice of medicinal chemistry*; Wermuth, C. G.; Aldous, D.; Raboisson, P.; Rognan, D., Eds.; Academic Press: San Diego, 2008; pp 539–559.
- (101) Oie, S. Drug distribution and binding. *J. Clin Pharmacol* **1986**, *26*, 583–586.
- (102) The Johns Hopkins University. *Animal care and use committee*; <https://web.jhu.edu/animalcare/> (accessed September 29, 2021).
- (103) Riches, A. C.; Sharp, J. G.; Thomas, D. B.; Smith, S. V. Blood volume determination in the mouse. *J. Physiol.* **1973**, *228*, 279–284.
- (104) Chapman, M. E.; Hu, L.; Plato, C. F.; Kohan, D. E. Bioimpedance spectroscopy for the estimation of body fluid volumes in mice, American journal of physiology. *Renal physiology* **2010**, *299*, F280–283.
- (105) Durbin, P. W.; Jeung, N.; Kullgren, B.; Clemons, G. K. Gross composition and plasma and extracellular water volumes of tissues of a reference mouse. *Health physics* **1992**, *63*, 427–442.

- (106) Rodell, C. B.; Arlauckas, S. P.; Cuccarese, M. F.; Garriss, C. S.; Li, R.; Ahmed, M. S.; Kohler, R. H.; Pittet, M. J.; Weissleder, R. TLR7/8-agonist-loaded nanoparticles promote the polarization of tumour-associated macrophages to enhance cancer immunotherapy. *Nat. Biomed Eng.* **2018**, *2*, 578–588.
- (107) AlSawaftah, N.; Pitt, W. G.; Hussein, G. A. Dual-Targeting and Stimuli-Triggered Liposomal Drug Delivery in Cancer Treatment. *ACS Pharmacol Transl Sci.* **2021**, *4*, 1028–1049.
- (108) Maeda, H.; Wu, J.; Sawa, T.; Matsumura, Y.; Hori, K. Tumor vascular permeability and the EPR effect in macromolecular therapeutics: a review. *J. controlled Release* **2000**, *65*, 271–284.
- (109) Torchilin, V. Tumor delivery of macromolecular drugs based on the EPR effect. *Adv. Drug Delivery Rev.* **2011**, *63*, 131–135.
- (110) Danaei, M.; Dehghankhold, M.; Ataei, S.; Hasanzadeh Davarani, F.; Javanmard, R.; Dokhani, A.; Khorasani, S.; Mozafari, M. R. Impact of particle size and polydispersity index on the clinical applications of lipidic nanocarrier systems. *Pharmaceutics* **2018**, *10*, 57.
- (111) Fraser, J. R.; Laurent, T. C.; Pertoft, H.; Baxter, E. Plasma clearance, tissue distribution and metabolism of hyaluronic acid injected intravenously in the rabbit. *Biochem. J.* **1981**, *200*, 415–424.
- (112) Trofymchuk, K.; Valanciunaite, J.; Andreiuk, B.; Reisch, A.; Collot, M.; Klymchenko, A. S. BODIPY-loaded polymer nanoparticles: chemical structure of cargo defines leakage from nanocarrier in living cells. *J. Mater. Chem. B* **2019**, *7*, 5199–5210.
- (113) Grossen, P.; Witzigmann, D.; Sieber, S.; Huwyler, J. PEG-PCL-based nanomedicines: A biodegradable drug delivery system and its application. *J. Controlled Release* **2017**, *260*, 46–60.
- (114) Saghatelian, T.; Tananyan, A.; Janoyan, N.; Tadevosyan, A.; Petrosyan, H.; Hovhannisyan, A.; Hayrapetyan, L.; Arustamyan, M.; Arnhold, J.; Rotmann, A.-R.; Hovhannisyan, A.; Panossian, A. Efficacy and safety of curcumin in combination with paclitaxel in patients with advanced, metastatic breast cancer: A comparative, randomized, double-blind, placebo-controlled clinical trial. *Phytomedicine* **2020**, *70*, 153218.
- (115) Matabudul, D.; Pucay, K.; Bolger, G.; Vcelar, B.; Majeed, M.; Helson, L. Tissue distribution of (Lipocurc) liposomal curcumin and tetrahydrocurcumin following two- and eight-hour infusions in Beagle dogs. *Anticancer research* **2012**, *32*, 4359–4364.
- (116) Storka, A.; Vcelar, B.; Klickovic, U.; Gouya, G.; Weisshaar, S.; Aschauer, S.; Bolger, G.; Helson, L.; Wolzt, M. Safety, tolerability and pharmacokinetics of liposomal curcumin in healthy humans. *International journal of clinical pharmacology and therapeutics* **2015**, *53*, 54–65.
- (117) Storka, A.; Vcelar, B.; Klickovic, U.; Gouya, G.; Weisshaar, S.; Aschauer, S.; Helson, L.; Wolzt, M. Effect of liposomal curcumin on red blood cells in vitro. *Anticancer research* **2013**, *33*, 3629–3634.
- (118) Du, M.; Shirabe, K.; Takeshita, M. Identification of alternative first exons of NADH-cytochrome b5 reductase gene expressed ubiquitously in human cells. *Biochem. Biophys. Res. Commun.* **1997**, *235*, 779–783.
- (119) Bolger, G. T.; Licollari, A.; Tan, A.; Greil, R.; Pleyer, L.; Vcelar, B.; Majeed, M.; Sordillo, P. Distribution of curcumin and THC in peripheral blood mononuclear cells isolated from healthy Individuals and patients with chronic lymphocytic leukemia. *Anticancer research* **2018**, *38*, 121–130.
- (120) Bolger, G. T.; Licollari, A.; Bagshaw, R.; Tan, A.; Greil, R.; Vcelar, B.; Majeed, M.; Sordillo, P. Intense uptake of liposomal curcumin by multiple myeloma cell lines: Comparison to normal lymphocytes, red blood cells and chronic lymphocytic leukemia cells. *Anticancer research* **2019**, *39*, 1161–1168.

Recommended by ACS

Lipid Nanoparticle (LNP) Chemistry Can Endow Unique *In Vivo* RNA Delivery Fates within the Liver That Alter Therapeutic Outcomes in a Cancer Model

Lindsay T. Johnson, Daniel J. Siegart, *et al.*

SEPTEMBER 26, 2022
MOLECULAR PHARMACEUTICS

READ 

Emerging Nanotechnologies and Microbiome Engineering for the Treatment of Inflammatory Bowel Disease

Omar A. Abed, James J. Moon, *et al.*

JULY 25, 2022
MOLECULAR PHARMACEUTICS

READ 

Intestinal Absorption of FITC-Dextran and Macromolecular Model Drugs in the Rat Intestinal Instillation Model

Staffan Berg, Christel A. S. Bergström, *et al.*

JUNE 01, 2022
MOLECULAR PHARMACEUTICS

READ 

Optimization of a Liposomal DNase I Formulation with an Extended Circulating Half-Life

Lesly Carolina Penaloza Arias, Davide Brambilla, *et al.*

MAY 11, 2022
MOLECULAR PHARMACEUTICS

READ 

Get More Suggestions >